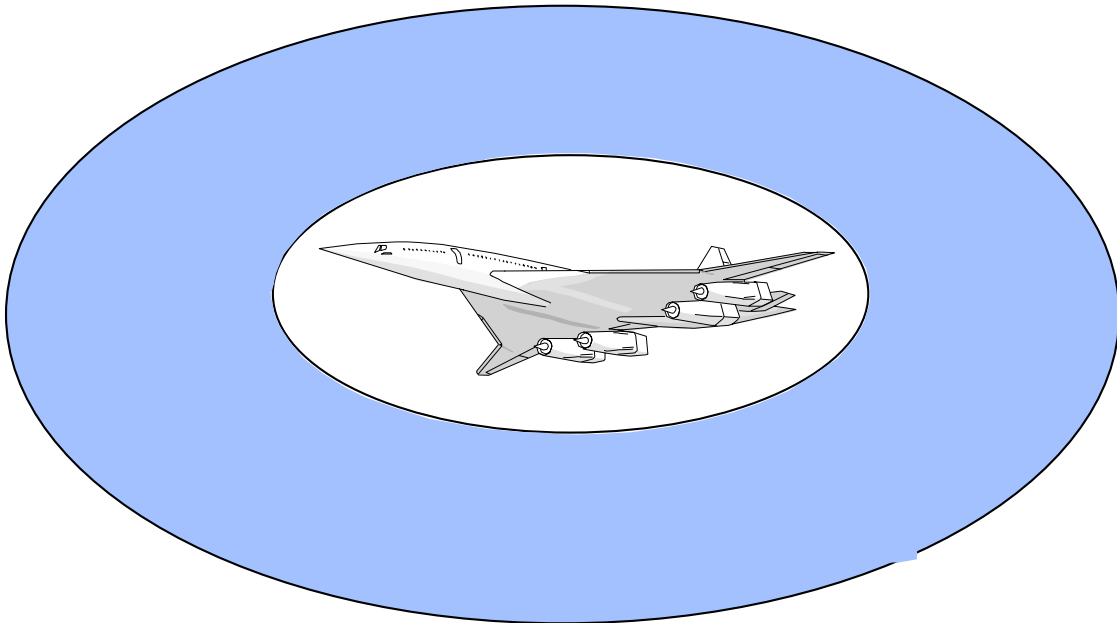


Configuration Aerodynamics Metric Update



Aerodynamics Performance Workshop

**NASA Langley
February 25 - February 28, 1997**

**Brenda M. Kulfan
Boeing Commercial Airplane Group**

Configuration Aero. Overview and Performance Metrics

- Overview of High Speed Aerodynamics HSR Tasks
 - Boeing 1997 Activities
- TCA Subsonic Cruise L/Dmax Projections
 - Review of “Tops Down” Process
 - TCA “Bottoms UP” Projection
- TCA Cruise L/Dmax Projections
 - Review of Process
 - Current Status
- CFD Methods / Processes Development Assessment
 - Define Stages of CFD Development”
 - Assess Current Capabilities
- Summary / Conclusions

The TCA cruise L/Dmax projection process will be reviewed. The current status of the non-linear designs of the TCA will be compared with the projections. Modifications to the projection process utilizing newly developed far-field optimization methods will be discussed. Examples of using these optimization methods to conduct design sensitivity studies will be shown.

The subsonic cruise “tops down” L/Dmax projection process will be reviewed. A “Bottoms Up” buildup of the TCA subsonic cruise L/D projections will be shown. The bottoms-up projections are shown to be consistent with the tops down projections.

The development and application of CFD design and analysis methods are critical to achieving a viable HSCT. The stages of CFD development will be discussed and related to the HSR technology levels. The current CFD design and analysis capabilities will be assessed.

The key points of this presentation will be summarized.

Topics

- TCA Cruise L/Dmax Projections
 - Review of Process
 - Current Status
 - Description of Modified Process
 - Examples of Design Sensitivity Studies
- TCA Subsonic Cruise L/Dmax Projections
 - Review of “Tops Down” Process
 - TCA “Bottoms UP” Projection
- CFD Methods / Processes Development Assessment
 - Define Stages of CFD Development
 - Relate to “Technology Readiness Levels”
 - Assess Current Capabilities
- Summary / Conclusions

designs of the TCA will be compared with the projections. Modifications to the projection process utilizing newly developed far-field optimization methods will be discussed. Examples of using these optimization methods to conduct design sensitivity studies will be shown.

The subsonic cruise “tops down” L/Dmax projection process will be reviewed. A “Bottoms Up” buildup of the TCA subsonic cruise L/D projections will be shown. The bottoms-up projections are shown to be consistent with the tops down projections.

The development and application of CFD design and analysis methods are critical to achieving a viable HSCT. The stages of CFD development will be discussed and related to the HSR technology levels. The current CFD design and analysis capabilities will be assessed.

The key points of this presentation will be summarized.

Importance of Accurate and Consistent Projections and Assessments

- Determine the Viability of an HSCT
- Define Meaningful Technology Development Goals
- Measure Technology Development Progress
- Proper focus of HSR Research Funds and Activities
- Support Correct Configuration Design Decisions

Current HSCT configuration studies are focused on determining the technical, economic and environmental viability of an High Speed Civil Transport. These studies must by necessity include projections of anticipated technical improvements for all of the key disciplines (e.g.. aerodynamic performance, structural materials and weights, propulsion system weights and performance, etc..). The projections represent current assessments of what is expected to be achievable with aggressive technology development programs.

The emerging developments in aerodynamic non-linear design and analysis methods offer the potential of significant improvements in aerodynamic cruise efficiency. These improvements will have a major effect on the viability of an HSCT.

It is essential to identify realistic achievable goals and to be able to measure the progress to achieve these goals. This is necessary to insure a properly focused technology developed program.

Technology Projection Approach



Tops Down Estimate

- Based on aerodynamic “fundamentals”
- Independent of initial or current aerodynamic performance
- Can apply process to any configuration
- Process is rigorous and consistent
- Useful for determining efficiency of initial design
- Projection is a **calculated** “achievable upper bound”

The “tops down” Approach”, which is used to project potential improvements in the supersonic cruise Lift/Drag ratio, is based on fundamental aerodynamic principles.

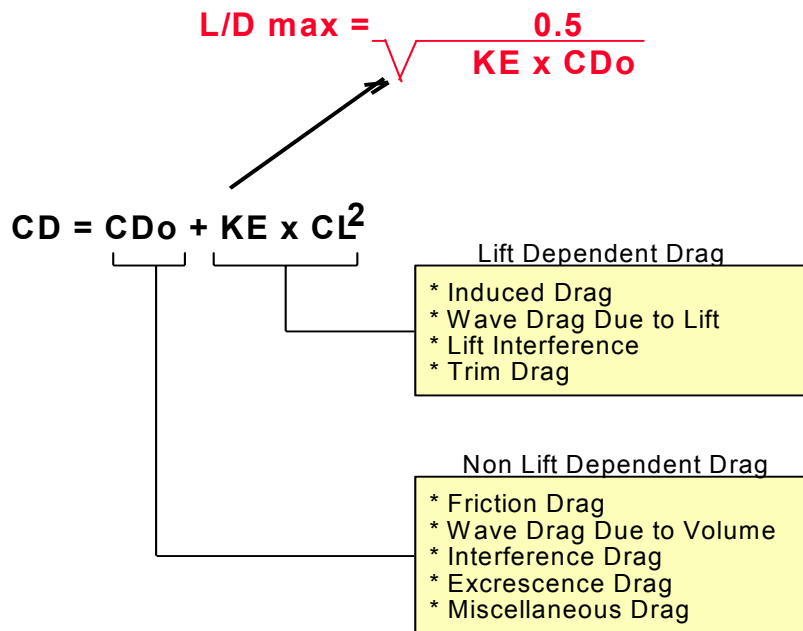
The projection does not depend on the current aerodynamic performance of specific configuration for which the projections are being made. They do, however, depend on the basic geometric features of the configuration.

The L/D projection is target level of L/D and is not a projected drag increment relative to the baseline configuration. However, a incremental drag improvement can be identified by comparing the projected drag level with the performance of the reference baseline design.

This is the approach that was presented in the reference, and will be briefly reviewed in this presentation. The process is both rigorous and consistent. The projection is a calculated “achievable” upper bound for L/Dmax.

Reference: Kulfan, Brenda M.; “Projecting and Tracking Advanced Technology Improvements in L/D”; Configuration Aerodynamics Workshop; NASA Langley 1966

Supersonic Drag Polar Approximation



The supersonic drag polar can be represented as a two term parabolic equation consisting of the non-lift dependent drag, CDo , plus the lift dependent drag $KE \times CL^2$.

The non-lift dependent drag includes:

- Friction drag
- Wave drag due to volume
- Volume interference drag
- Excrescence and other miscellaneous drag items.

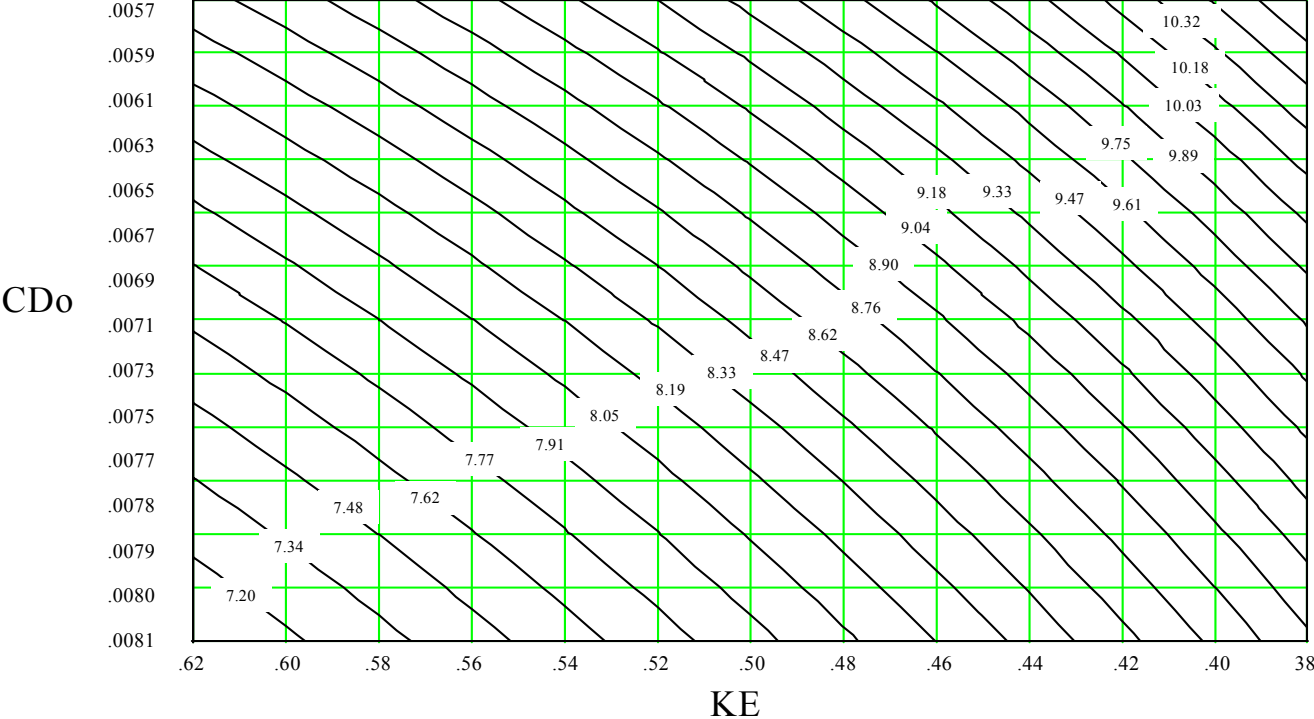
The lift dependent drag consists of :

- Induced drag
- Wave drag due to lift
- Lift interference effects
- Trim drag.

Based on the parabolic drag polar representation, it can be shown that L/D_{max} varies inversely with the square root of the product of CDo and the drag due to lift factor KE .

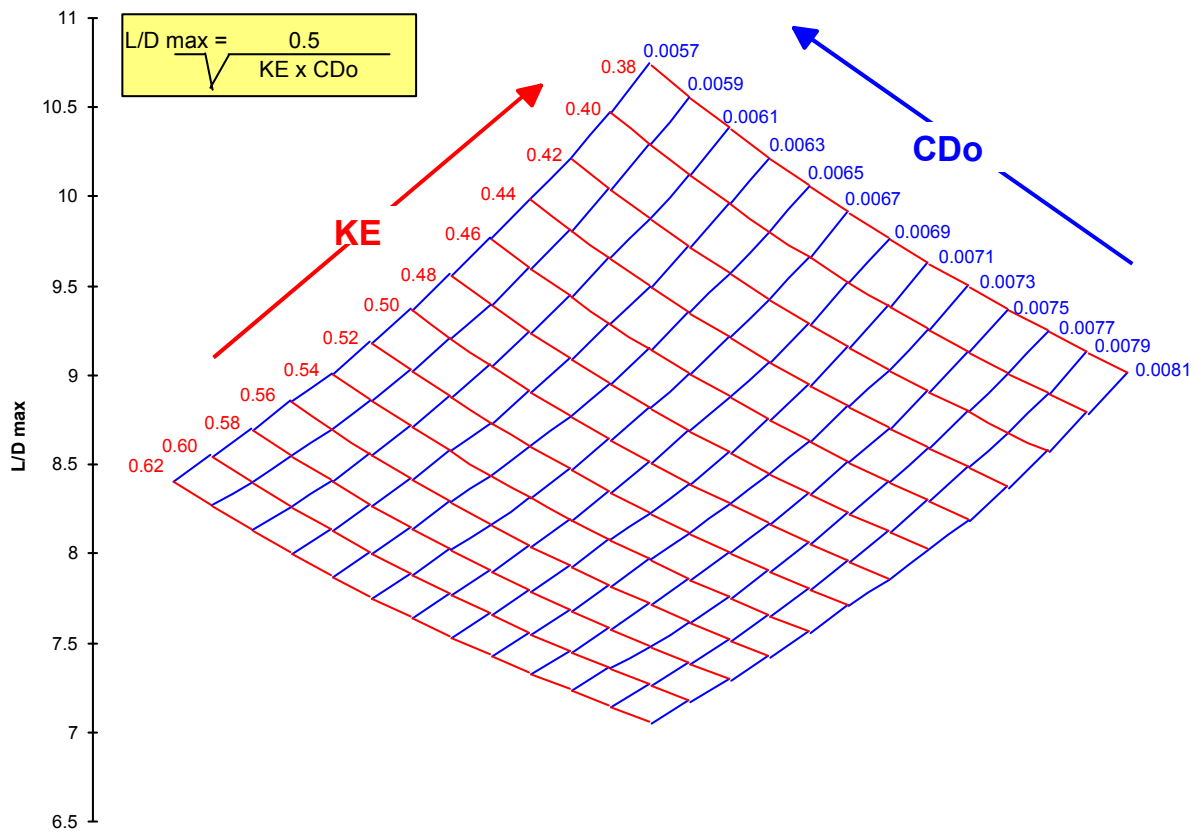
HSCT AERODYNAMIC PERFORMANCE DESIGN SPACE

L/D max Contour Plot



L/Dmax contours can be calculated for various values of KE and CDo to map out the potential design space for a supersonic configuration.

HSCT Aerodynamic Performance Design Space



A more convenient way to view the dependency of L/Dmax on CDo and KE is in the form of a carpet plot. This is the form that we will use to develop the region for acceptable designs of a specific configuration. This is a two dimensional representation of the design space for supersonic configurations.

In the discussions that follow, it is assumed that the gross overall features of any configuration remain fixed. These include such things as wing area, wing volume, location on the wing on the body, body volume, nacelle overall size and locations, and planform shape. What we wish to determine is the region of acceptable designs that could be developed by different design methods and techniques. We will then determine what is considered to be the overall upper limit of achievable L/Dmax for that specific configuration. To do this we will identify values of CDo and KE that are considered too high for an acceptable design. We will then use fundamental aerodynamic concepts to determine lower bounds of achievable CDo and KE.

CD₀ “TOO HIGH” LIMIT FOR ACCEPTABLE DESIGN

$$CD_0 < CD_F + \sum CD_{WISOL} + CD_{MISC} + CD_{EXCRES}$$

- FULLY TURBULENT FRICTION DRAG
- SUM OF COMPONENT ISOLATED WAVE DRAG
[NO FAVORABLE INTERFERENCE]
- CURRENT TECHNOLOGY EXCRESCENCE AND MISCELLANEOUS DRAG
- *** DRAG CAN BE WORSE THAN THIS ***

CD₀ is considered “too high” if the non-lift-dependent drag exceeds the sum of:

- CDF = Fully turbulent flow flat plate skin friction drag.
- CDW = The sum of the isolated wave drag of each of the configuration components. This corresponds to a design with no net favorable aerodynamic interference.
- CDmisc = Current technology miscellaneous drag including excrescence drag.

The most common causes of CD₀ being too high are:

- Unfavorable wing / body interference drag for a non-area-ruled body.
- Nacelles designed and / or located to produce volume wave drag interference.
- Large out of contour bumps such as landing gear fairings
- Separated flow over the wing upper surface or in the vicinity of the nacelle / diverter intersection with the wing.

The zero lift drag can actually be worse than this acceptable upper limit for CD₀.

KE “ TOO HIGH ” LIMIT FOR ACCEPTABLE DESIGN

$$KE < KE_{S=0}$$

- EQUIVALENT TO DRAG OF FLAT WING CONFIGURATION
- NO TRIM DRAG
- NO LIFT INTERFERENCE DRAG
- *** DRAG CAN ACTUALLY BE HIGHER ***

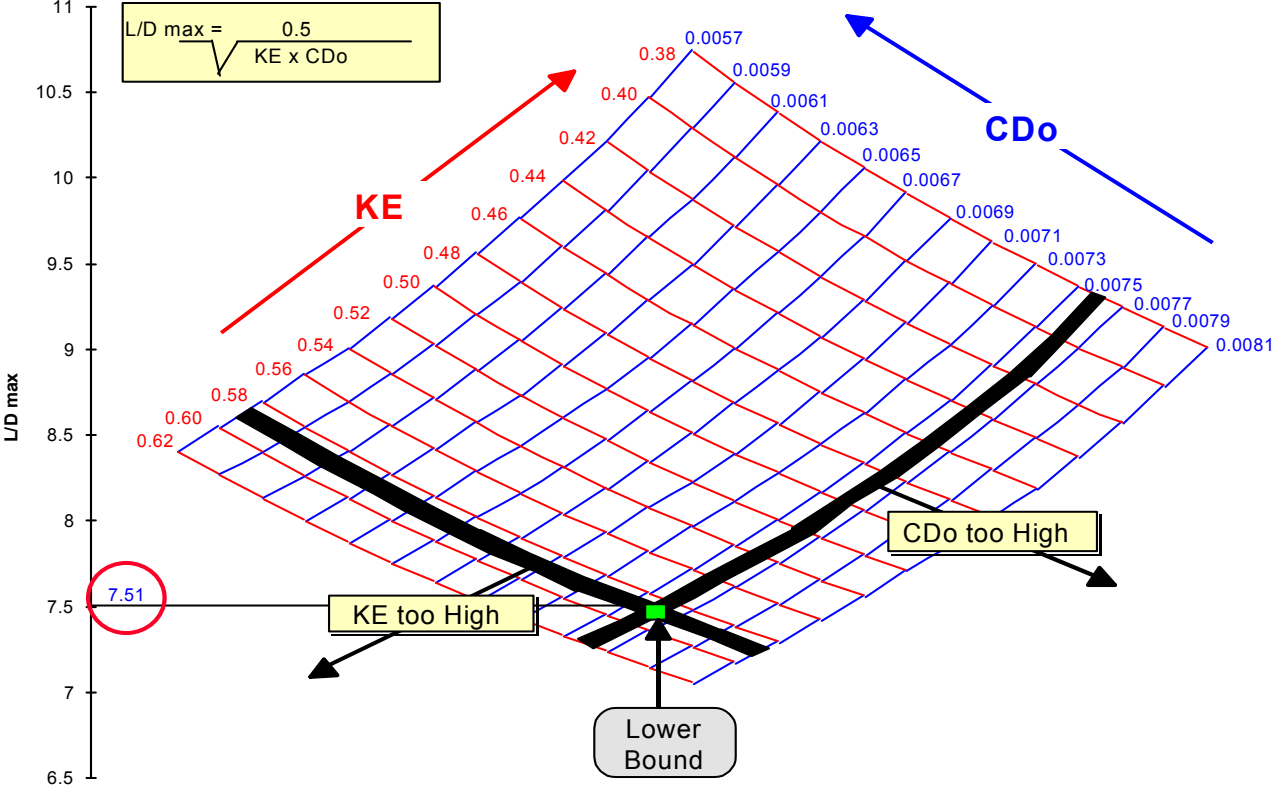
As an upper limit for KE we assume that the drag due to lift should be no worse the drag of a thin flat symmetric wing design with no leading edge suction.

We also assume no favorable interference lift or trim drag.

Again the drag for a very poor design can exceed this limit

Lower Bound for L/D max

Typical HSCT Mach = 2.4



The intersection of the “ C_{Do} too high” boundary and the “KE too high” boundary determines the lower bound for L/D_{max} . This lower bound for L/D_{max} essentially corresponds to the Concorde aerodynamic efficiency level.

CD₀ “TOO LOW” LIMIT

$$CD_0 > CD_F + 1.75 CD_{W SH}$$

- FULLY TURBULENT FLAT PLATE SKIN FRICTION
- WING / BODY WAVE DRAG = 1.75 X EQUIVALENT SEARS-HAACK BODY
- ZERO INSTALLED NACELLE WAVE DRAG
- EMPENNAGE WAVE DRAG INCLUDED IN WING / BODY WAVE DRAG
- *** DRAG “CAN’T” BE LOWER THAN THIS ***

The “too low” limit for zero lift drag is equal to the sum of:

- Fully turbulent skin friction drag
- Wing / body volume wave drag equal to 1.75 times the drag of an equivalent Sears-Haack body having the same maximum area as the combined wing plus body area distribution and the length of the fuselage. The empennage drag is included as part of the wing / body drag.
- Zero installed nacelle wave drag

The zero lift “can’t be lower” than this level for the given configuration.

KE “TOO LOW” LIMIT

$$KE > KE_{S=1} \{ KE_{FAC} - 2 K_{NAC} (DCL_N/CL) - K_{TRIM} (KE_{S=1}/K_{TAIL}) (S_{HT}/S_{REF}) \}$$

- WING / BODY KE 5% LOWER THAN “FULL SUCTION” DRAG LEVEL ==>
 $KE_{FAC} = 0.95$
- FAVORABLE LIFT INTERFERENCE : 625% OF “IDEAL” ==> $K_{NAC} = 0.625$
- FAVORABLE TRIM DRAG : 70% OF “IDEAL” ==> $K_{TRIM} = 0.70$

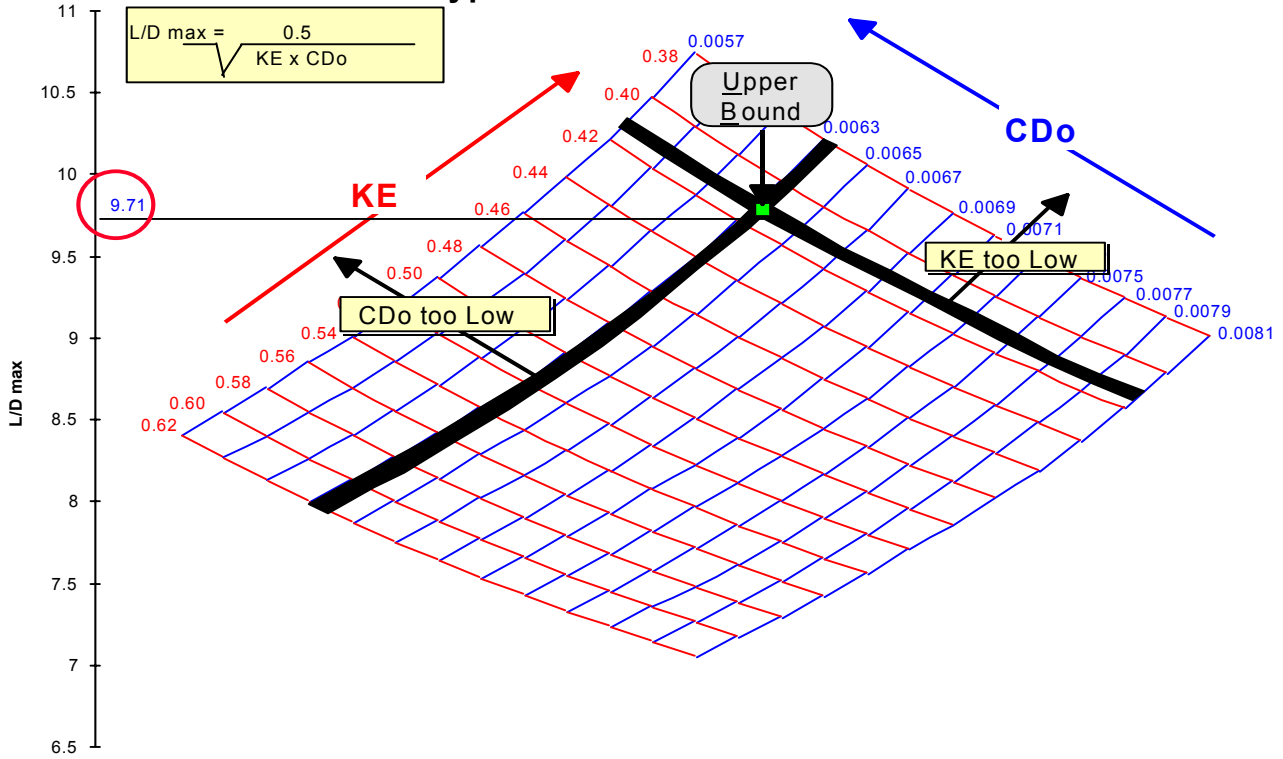
The achievable wing / body drag due to lift level used in the initial projection process is equal to 95% of the flat wing with full leading suction.

Nacelles designed properly to produce a positive pressure field on the lower surface of the wing can create a favorable interference lift that reduces the necessary wing / body lift for a given overall lift coefficient. This results in a reduction in wing / body drag due to lift. However, the nacelle pressure field acting on the wing camber surface produces a drag increment and the the wing lifting pressures acting on the nacelles produce an adverse buoyancy drag. On current nacelle installations about half of the ideal lift interference favorable interference is lost because of these two adverse effects. For the lower limit drag due to lift we assume that it is possible to achieve 65% of the ideal nacelle lift interference effects.

At supersonic speeds a horizontal tail upload will also result in a reduction in drag due to lift. The ideal level occurs when the tail upload is not reduced by any wing downwash effects. A favorable trim drag equal to 70% of the ideal level is considered to be achievable.

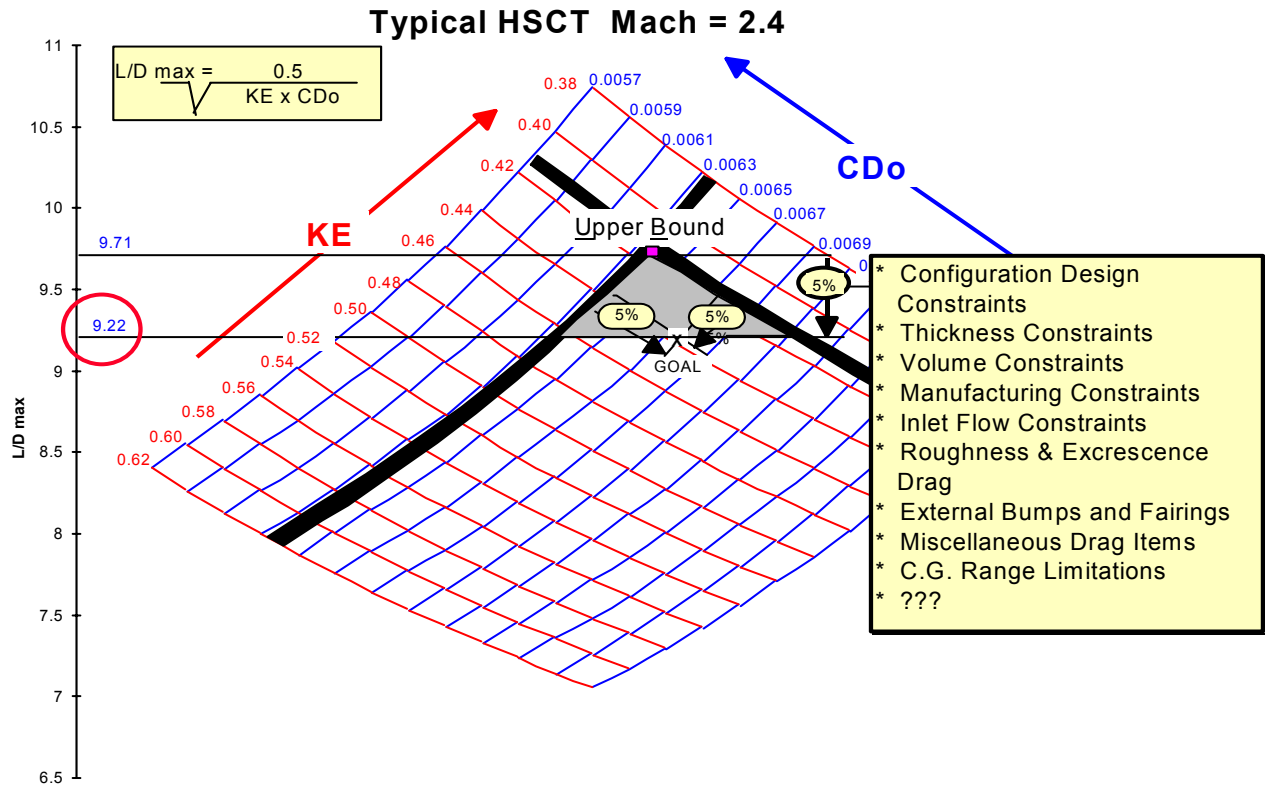
Upper Bound for L/D max

Typical HSCT Mach = 2.4



The intersection of the CDo “too low” boundary with the KE “too low” boundary defines the upper bound for L/Dmax

Realistic Goal for L/D max Improvements



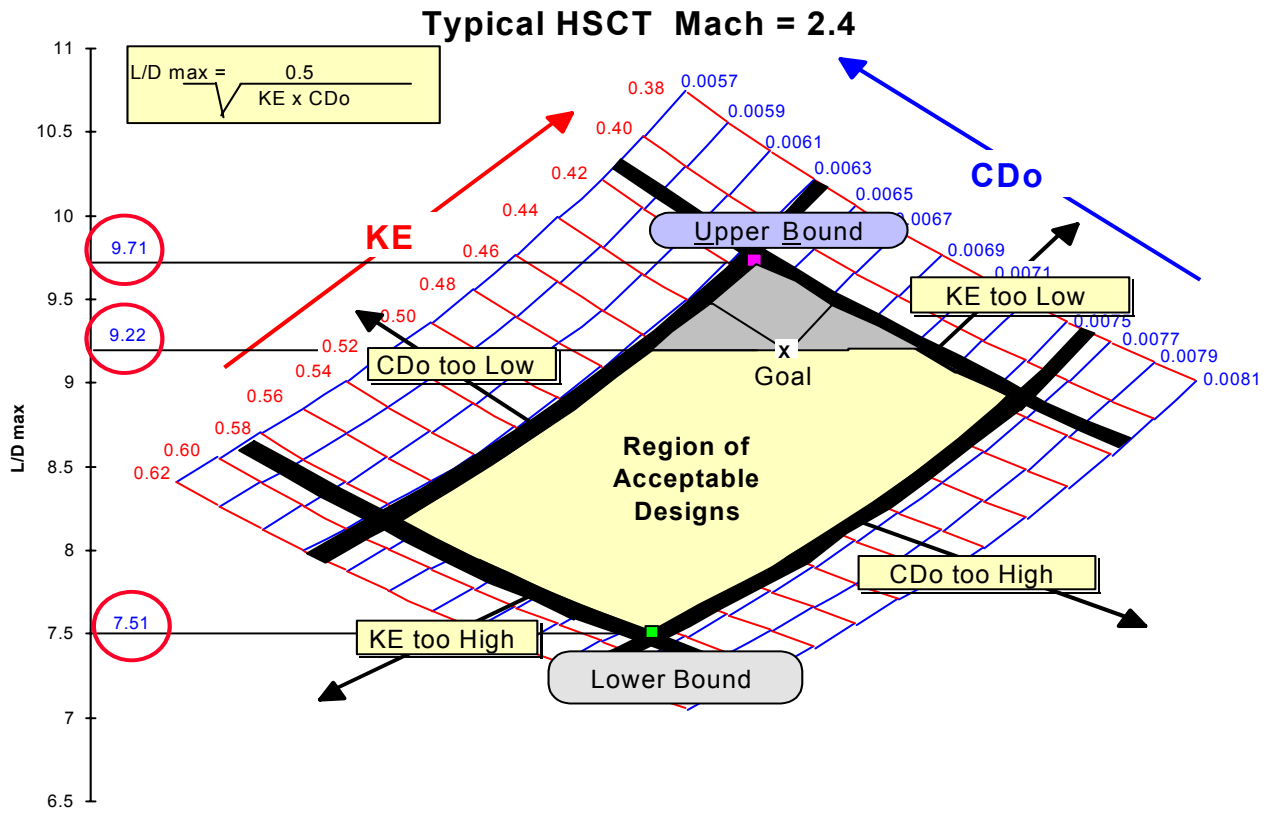
The upper bound level for L/Dmax is not achievable because of practical configuration design considerations and constraints.

These constraints for a supersonic transport aircraft include such factors as:

- Configuration thickness and volume constraints
- Manufacturing and surface curvature constraints
- Inlet flow constraints
- Ground clearance effects on aftbody upsweep
- External bumps and fairings
- Roughness and excrescence drag
- Cruise center cg gravity limitations
- Miscellaneous drag items

A “goal” L/Dmax equal to 95% of the achievable L/Dmax is used to account for these effects.

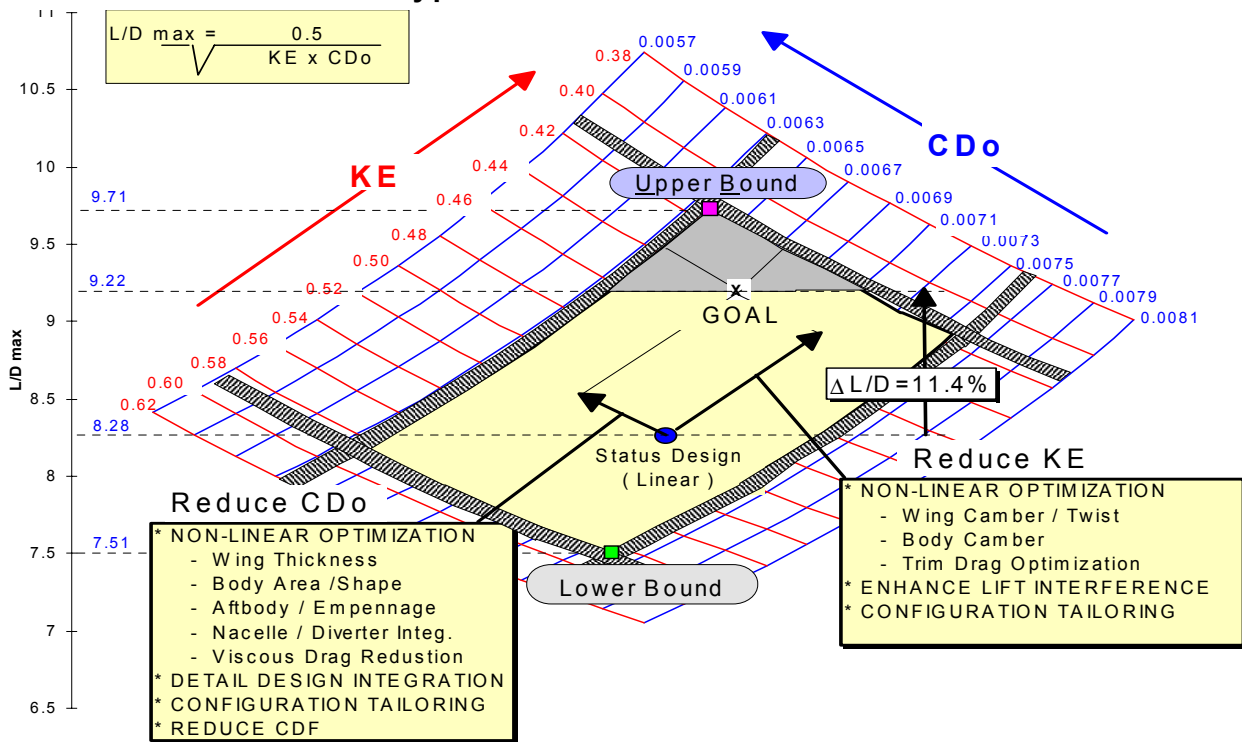
Region of Acceptable Designs



Combining the upper and lower boundaries for zero lift drag, CDo, and for drag due to lift factor, KE, defines the region for acceptable designs of a specific configuration.

Opportunities for L/D max Improvements

Typical HSCT Mach = 2.4

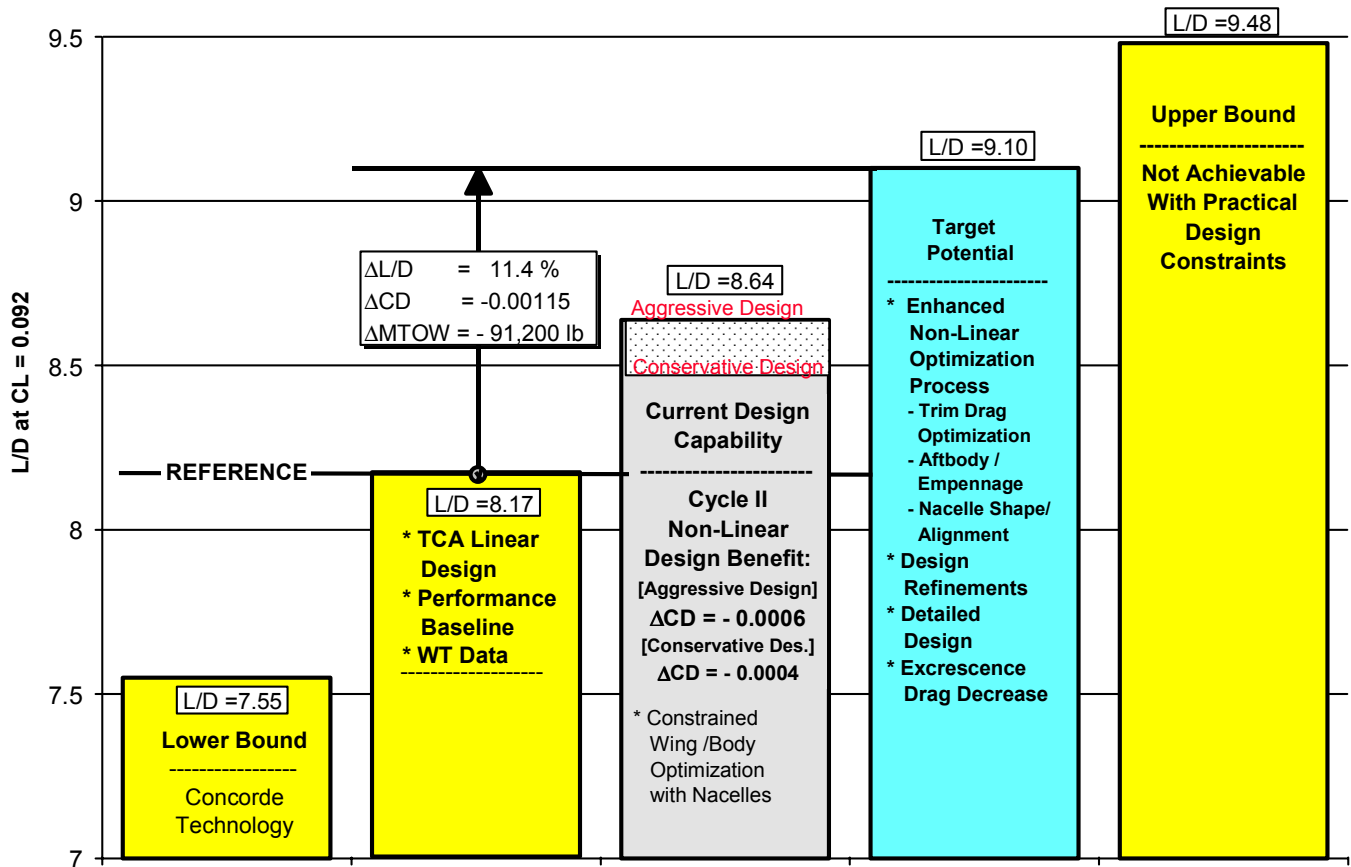


The difference between the goal L/Dmax level and the L/Dmax of the linear theory status design is the projected benefit of design optimization and design development using the emerging advanced nonlinear design and analysis methods relative to the baseline configuration.

The figure includes factors that are expected to contribute to reductions in both CDo and the drag due to lift factor, KE.

TCA Cruise L/Dmax Projections

Mach = 2.4 CL= 0.092



This figure shows the impacted of the projected improvements in cruise L/Dmax on the MTOW of the mission sized HSCT configuration relative to the current linear design. The 11.4% projected improvement in L/Dmax will result in a reduction in the maximum takeoff weight of 91,200 lbs.

The results of the recently completed cycle II non-linear design optimization by the Configuration Aerodynamics team has defined a conservative design having a 4 count drag reduction relative to the linear TCA baseline and more aggressive designs that have 6 counts lower drag than the baseline.

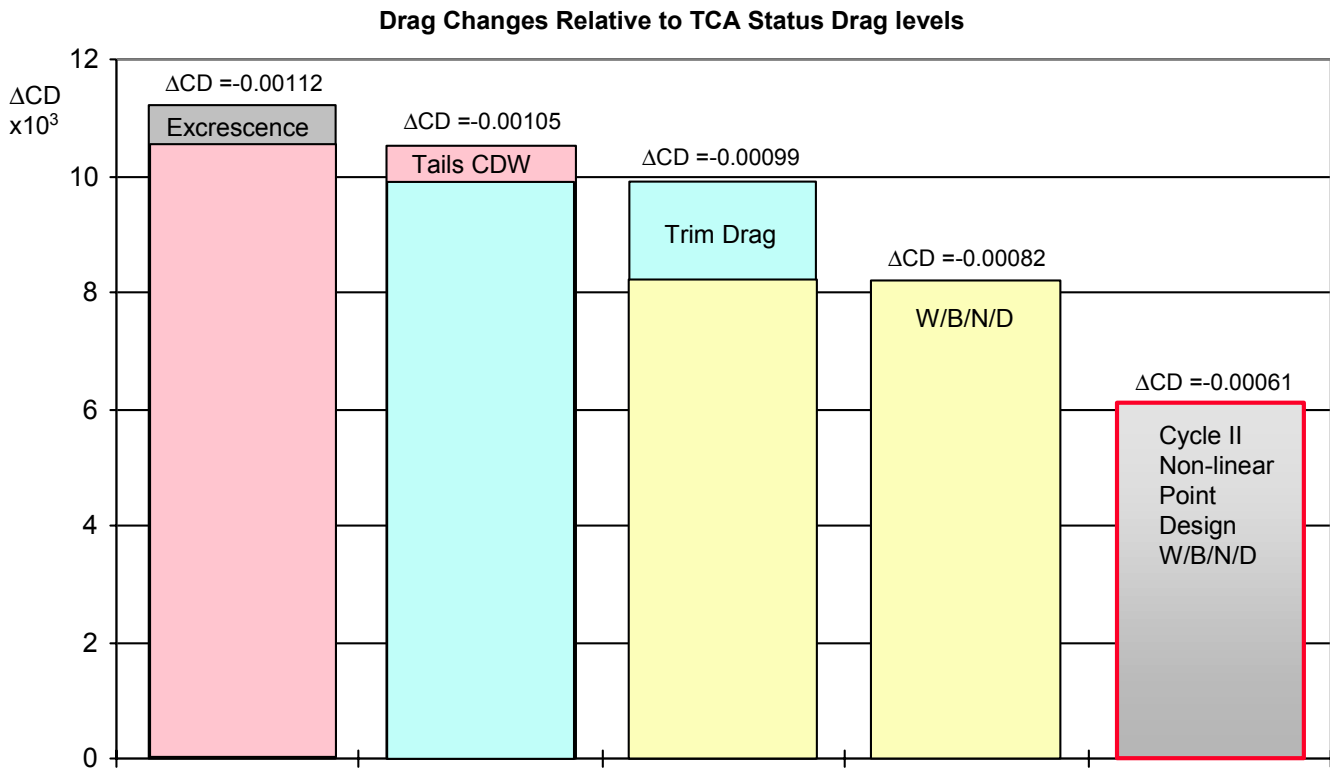
The projected further improvements in L/D max will result further developments and enhancements in the emerging non-linear aerodynamic design optimization technology together with improvements in detailed design. Examples of anticipated improvements in the detailed design processes include:

- Nacelle / diverter design integration
- Landing gear design integration
- Wing / body junction design
- Viscous and excrescence drag reduction
- Trim drag optimization
- Aftbody and empennage design,

TCA L/Dmax Projection Drag Components

Mach = 2.4

CL - 0.092



This shows the breakdown of the components of the projected drag improvements relative to the baseline TCA.

These include:

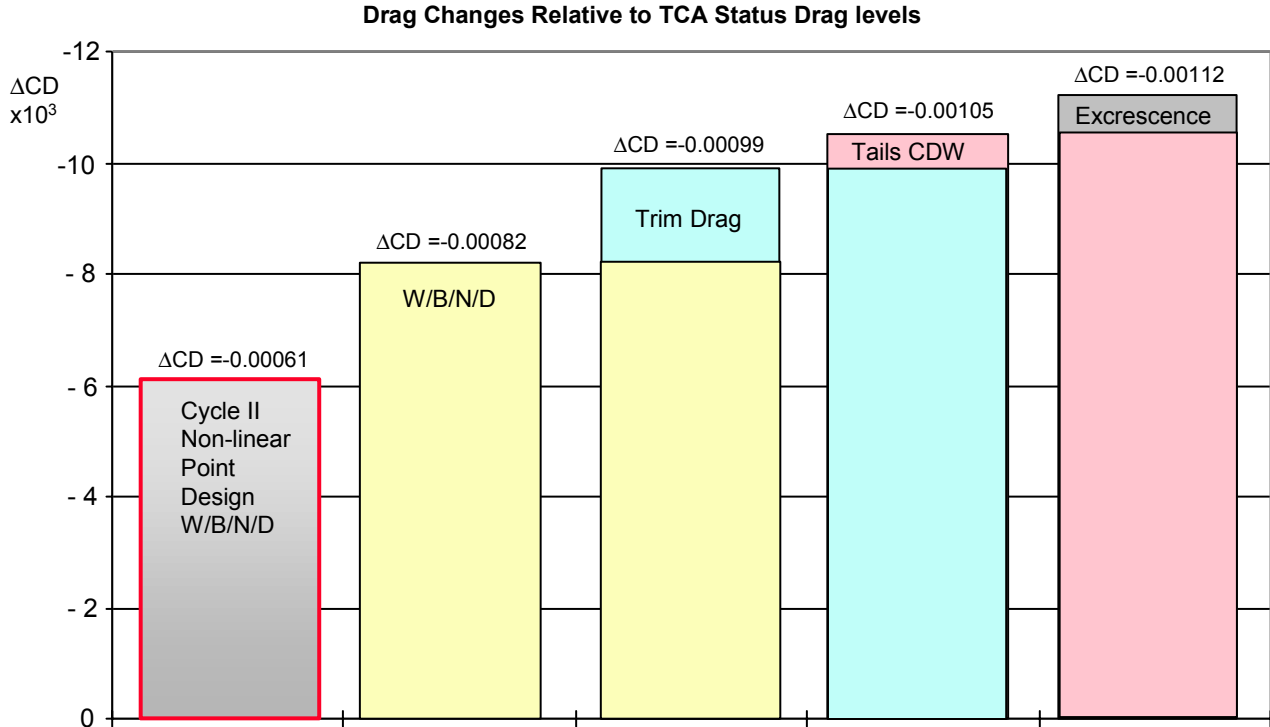
- Excrescence Drag reduction: $X\Delta = - 0.00007$
- Aftbody / empennage wave drag reduction: $X\Delta = - 0.00006$
- Trim drag reduction: $X\Delta = - 0.00017$
- Wing / body / nacelle / diverter drag reduction: $X\Delta = - 0.00082$

The current cycle II optimized wing / body designs have already achieved much of the anticipated gain for wing / body / nacelle / diverter design integration and optimization.

TCA L/Dmax Projection Drag Components

Mach = 2.4

CL - 0.092



This shows the breakdown of the components of the projected drag improvements relative to the baseline TCA.

These include:

- Excrescence Drag reduction: $X\Delta = - 0.00007$
- Aftbody / empennage wave drag reduction: $X\Delta = - 0.00006$
- Trim drag reduction: $X\Delta = - 0.00017$
- Wing / body / nacelle / diverter drag reduction: $X\Delta = - 0.00082$

The current cycle II optimized wing / body designs have already achieved much of the anticipated gain for wing / body / nacelle / diverter design integration and optimization.

Projection Process Modifications

- REPLACE CAW LOWER LIMIT CRITERIA BY NEW FAR FIELD VOLUME WAVE DRAG OPTIMIZATION PREDICTIONS

- REPLACE KE LOWER LIMIT CRITERIA BY NEW FAR FIELD LIFT WAVE DRAG PLUS INDUCED DRAG OPTIMIZATION PREDICTIONS

The original projection process is adaptable to further enhancements.

We have recently developed a new and unique method to use far field linear theory to calculate minimum wing / body volume wave drag, and minimum lift wave drag plus induced drag.

These predictions will be incorporated in the revised projection process.

Modified CDo “TOO LOW” LIMIT

- REPLACE 1.75x(CDw sh) LOWER LIMIT CRITERIA BY NEW FAR FIELD VOLUME WAVE DRAG W/B/N/T OPTIMIZATION PREDICTIONS

$$CDo > CD_F + (CD_W)_{Lb}$$

- FULLY TURBULENT FLAT PLATE SKIN FRICTION
- WING / BODY / NACELLE CALCULATED CONSTANT VOLUME MINIMUM WAVE DRAG
- EMPENNAGE CALCULATED CONSTANT VOLUME MINIMUM WAVE DRAG
- *** DRAG “CAN’T” BE LOWER THAN THIS ***

In the modified projection process the wing / body / nacelle / empennage minimum wave drag is determined using the new far-field optimization method keeping nacelle shape, body length and volume, wing volume, tail volume all constant.

KE “TOO LOW” LIMIT

- REPLACE “0.95 x KE_{S=1}” LOWER LIMIT CRITERIA BY NEW FAR FIELD INDUCED DRAG PLUS LIFT WAVE DRAG OPTIMIZATION PREDICTIONS

$$KE > (KE_{ID} + KE_{WDL})_{OPT} \{ 1 - 2 K_{NAC} (\Delta CL_N / CL) - K_{TRIM} (KE_{S=1} / K_{TAIL}) (S_{HT} / S_{REF}) \}$$

- WING / BODY KE = LOWER BOUND OF INDUCED DRAG PLUS LIFT WAVE DRAG
- FAVORABLE LIFT INTERFERENCE : 625% OF “IDEAL” ==> $K_{NAC} = 0.625$
- FAVORABLE TRIM DRAG : 70% OF “IDEAL” ==> $K_{TRIM} = 0.70$

The wing / body drag due to lift is calculated as the minimum sum of induced drag plus wave drag due to lift including nacelle lift interference effects.

New Projection Process Serendipities

- Greater Insight into Sources of Drag Improvement
- Assessment of Impact of Design Constraints
- Rapid Design Sensitivity Studies
- Determine Optimum Lift Distribution and Sensitivity to Pitching Moment Constraint

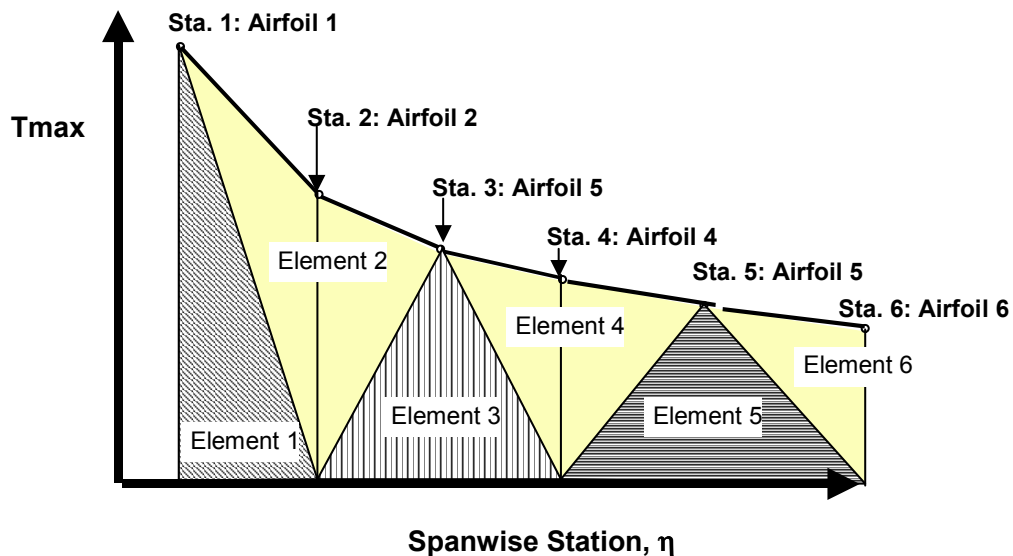
The new projection process currently being developed will offer a number of serendipities including:

- Greater insight into the sources of potential drag improvement
- Assessment of the impact of various design constraints
- Rapid sensitivity studies can be conducted
- The optimum lift distribution is defined
- Sensitivity to pitching moment constraint.

Wing Fundamental Triangular Elements

- The Wing Thickness Variation Can Be Represented by Fundamental Triangular Elements.
- Each Element is Defined by It's Central Airfoil, A_i for $i=1$ to N
- The Wing Section Between Adjacent Airfoils is Defined by Linear Variation of Thickness Along Constant Percent Chord Lines.
- The Volume of the Wing is Equal to the Sum of the Volumes of the Individual Elements

$$Vol = \sum_{i=1}^N k_i \Delta V_i$$



This illustrates the new far field wave drag optimization process.

The wing thickness distribution can be represented by a series of airfoils at a number of stations across the wing span. The thickness is allowed to vary linearly between adjacent airfoils along constant percent chord lines.

Each airfoil therefore contributes only to a triangular element of the wing. The total wing volume is the sum of the volumes of the triangular elements.

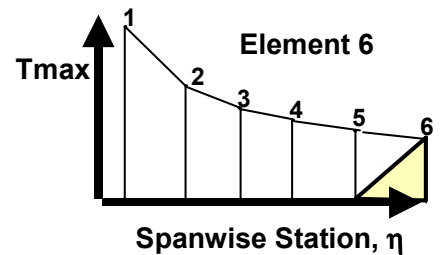
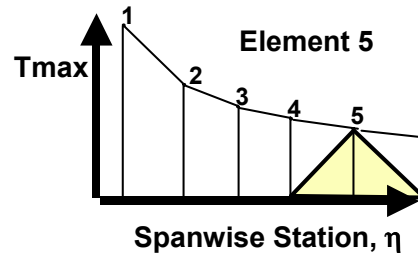
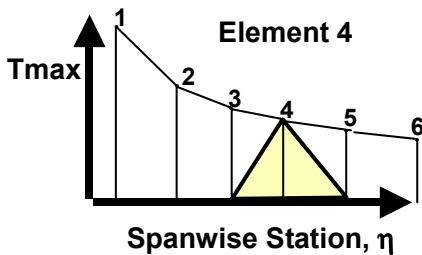
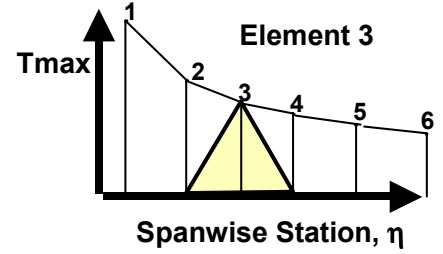
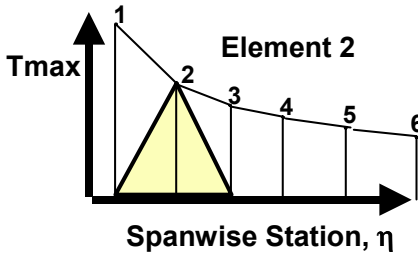
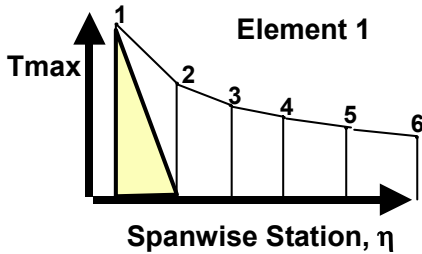
At each airfoil station, the airfoil can also be represented as a sum of fundamental airfoil shapes.

Wing Drag Calculation Using Fundamental Elements

The Wave Drag of the Wing Can be Calculated as the Sum of:

- The Drag of Each of the Isolated Elements, CD_{II}
- The Interference Drag Between Each Individual Pair of Elements, CD_{IJ}

• The Total Drag is: $CD = \sum_{I=1}^N \sum_{J=1}^N k_I k_J CD_{IJ}$



The wave drag of the wing can be calculated as the sum of the wave drags of the fundamental elements plus the interference drag between each pair of elements.

The optimization process determines the optimum scaling of each fundamental airfoil at each airfoil station that will minimize wave drag of the wing while maintaining constant wing volume. Interference effects of the nacelles and the body on the wing elements are also included.

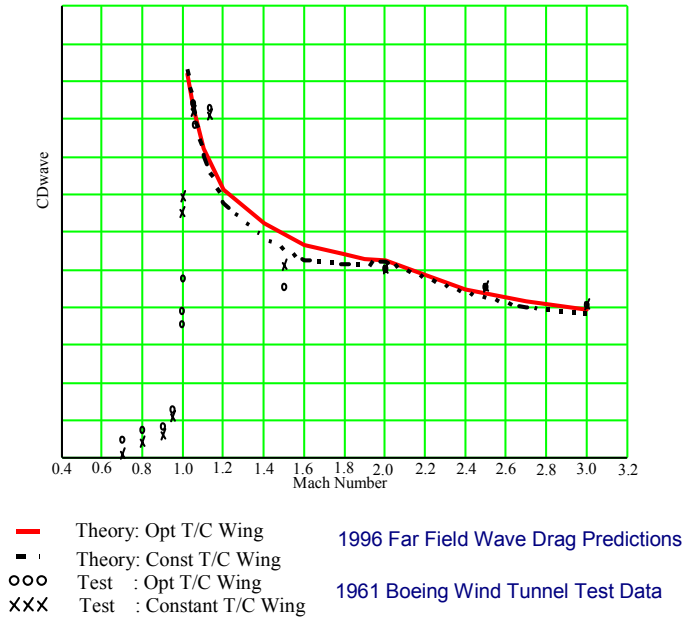
Wing thickness / depth constraints can also be included, but are not when determining the lower bound wave drag.

COMPARISON OF TEST vs THEORETICAL WAVE DRAG

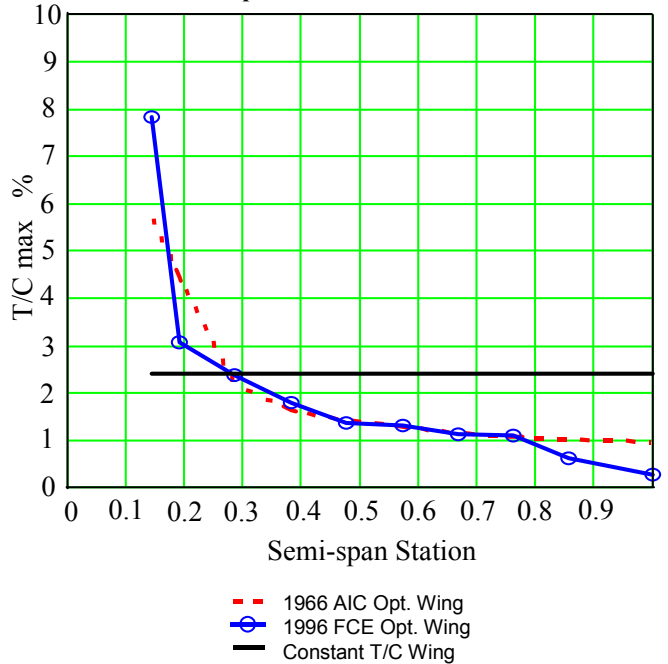
Optimum T/C Wing = 44.8 in³ (+18.8%)
 Constant T/C Wing Volume = 37.7 in³

Test vs Theory Wing + Body Wave Drag

Theoretical CDF Removed From Test Data



Comparison of T/C Max Distributions



This new optimization method was validated by comparison with historic wind tunnel data from a wing thickness optimization study that was conducted using the aerodynamic influence coefficient method that was the forerunner of today's modern CFD codes. The spanwise thickness distribution of a simple delta wing mounted on an ogive / cylinder body was optimized to maximize wing volume for constant wave drag at a cruise Mach number of 3.0

The reference constant t/c wing and optimized wings were both built and tested in the Boeing supersonic wind tunnel.

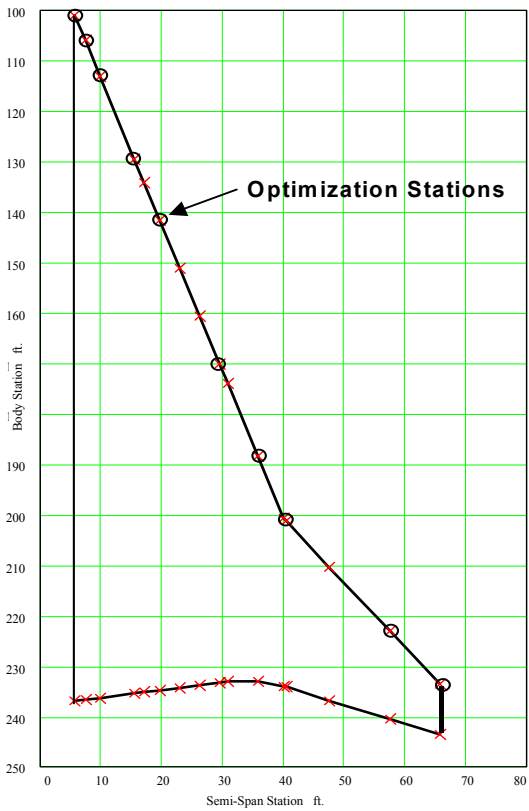
The figure on the left compares predicted and measured zero lift drags for the optimized and reference wings. Theoretical friction drag was removed from the test data. The farfield wave drag predictions match the test data quite well.

The figure on the right compares the optimized thickness distribution calculated by the new fundamental composite element method (FCE) with that determined by the original aerodynamic influence coefficient (AIC) method. The FCE wave drag is actually slightly lower than the AIC design. The thickness distributions differ near the wing root and wing tip where the AIC design had been modified to produce a more realistic wind tunnel model design.

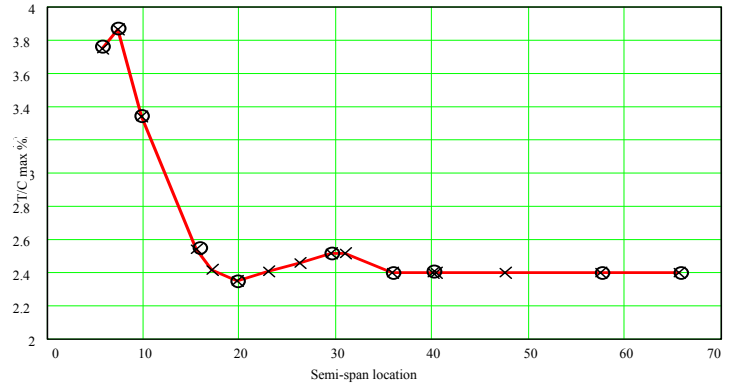
Subsequent sensitivity studies by the new FCE method indicated negligible changes in drag with these modifications.

TCA Planform and Thickness Distribution

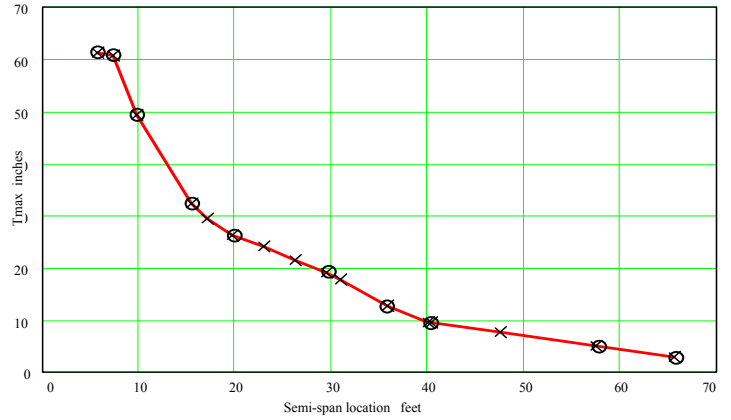
TCA Planform



Maximum Thickness/ Chord Ratio



Maximum Thickness

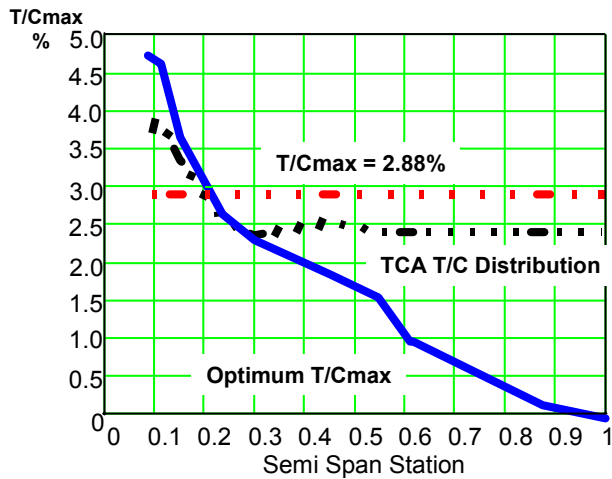


The fundamental composite element wave drag optimization method was applied to the baseline TCA configuration. In this original application, the airfoil shapes were held constant and the spanwise thickness distribution was optimized.

The figure shows the TCA planform and the wing optimization stations.

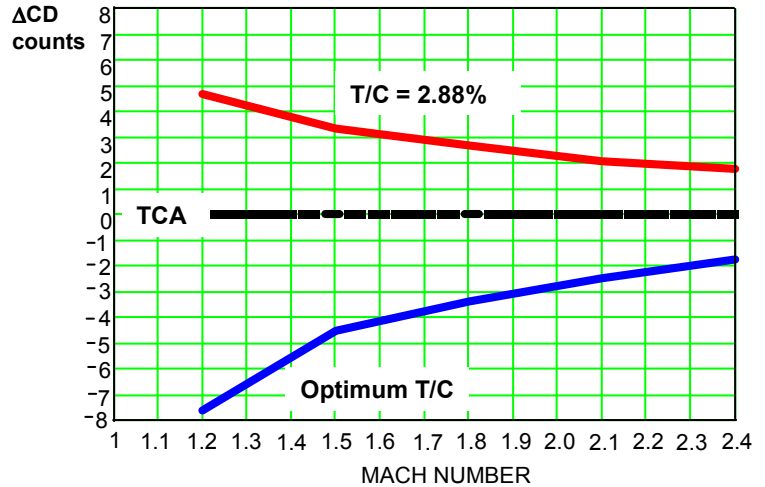
TCA T/C Distribution Study

- * Isolated Wing
- * Constant Wing Volume
- * Mach = 2.4



- TCA T/C Distribution
- Optimum T/C Distribution
- Constant T/C Wing

• Isolated Wing Drag Relative to TCA T/C Distribution

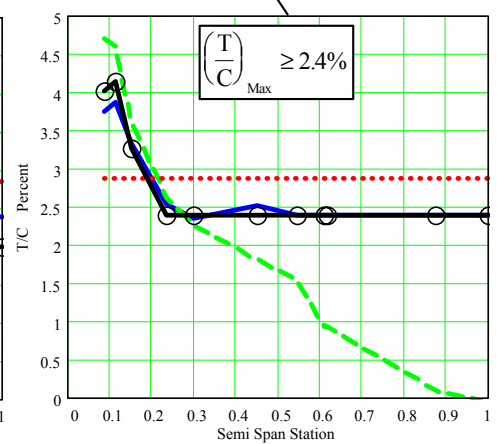
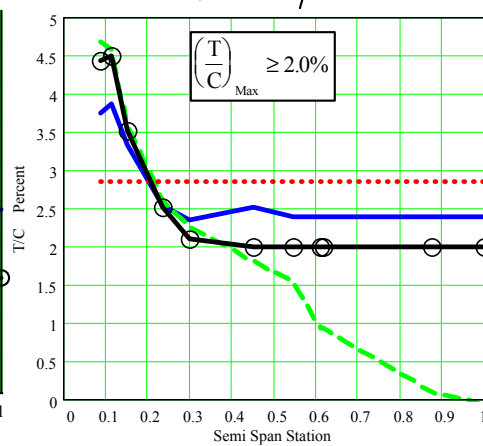
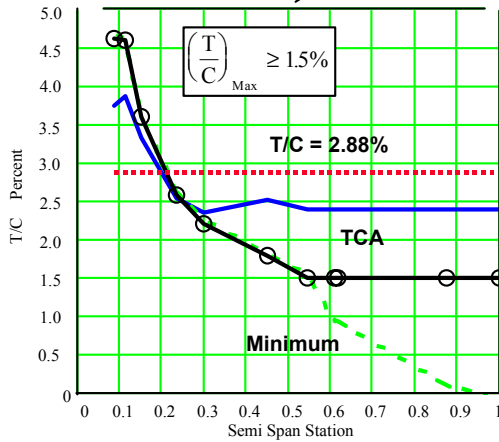
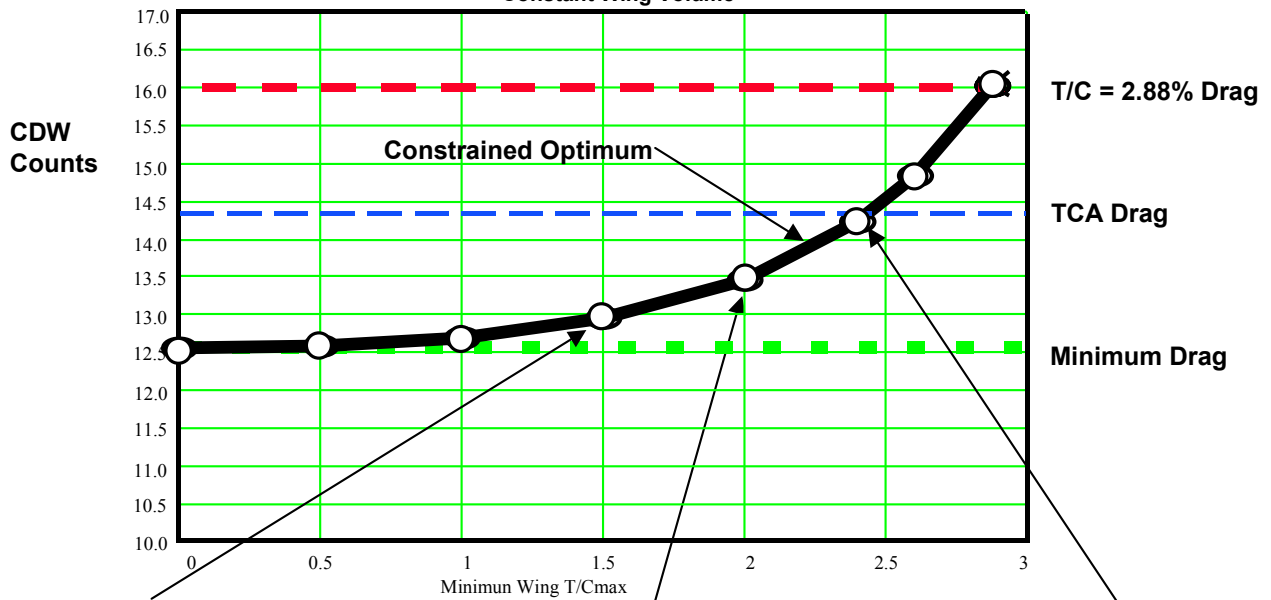


This shows the results of the TCA spanwise thickness optimization study. The TCA thickness distribution is compared with the optimized thickness distribution and with a constant T/C wing having the same airfoil shapes and wing volume. The optimized wing does not “like” the supersonic portion of the wing and tries to eliminate it by reducing the wing thickness to zero near the wing tip and increasing the thickness near the wing root.

The figure on the right shows the wave drag increments of the optimized design and the constant T/C wing relative to the TCA. Even though the design Mach number was 2.4, significant drag reduction was achieved across the entire supersonic Mach range.

Effect of T/Cmax Constraint on TCA Isolated Wing Wave Drag

- Mach = 2.4
- Constant Wing Volume



This shows the results of optimized wing sensitivity studies in which minimum T/C was constrained. For each minimum T/C constraint the wing was optimized to minimize the wave drag subject to the constrained T/C value.

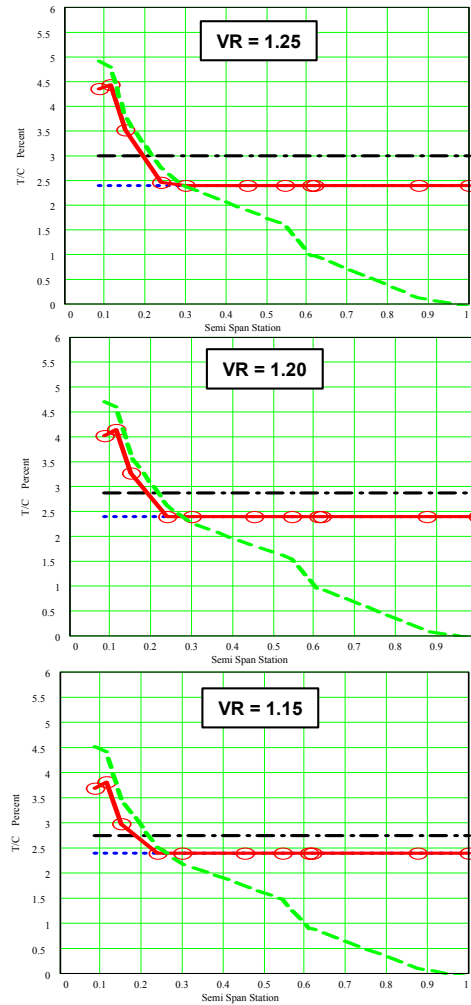
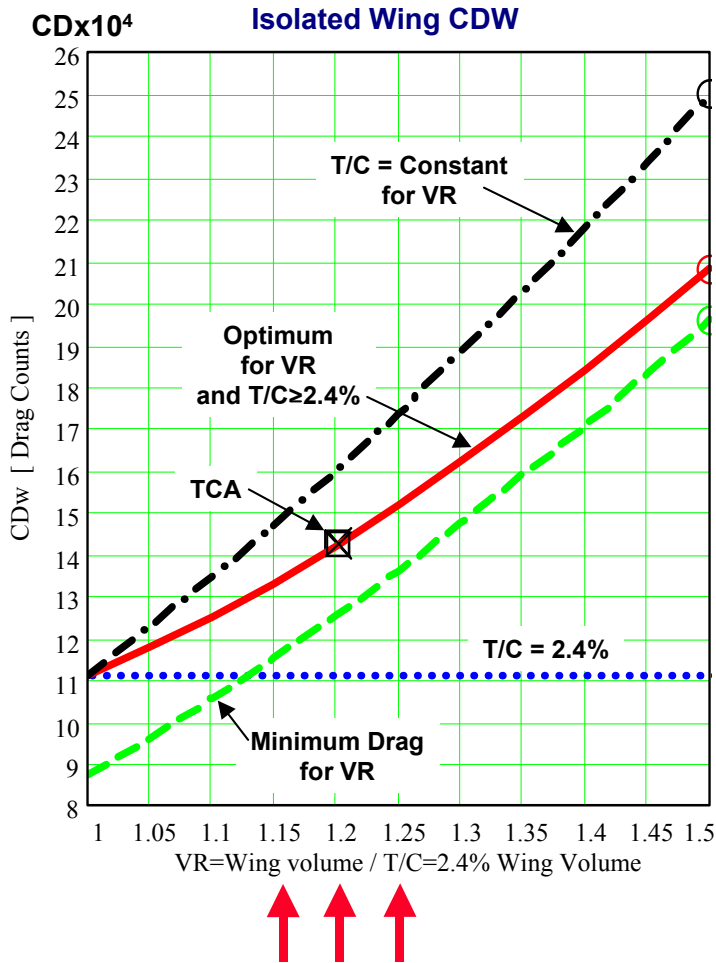
The minimum wing T/C can be increased to 1.5% for less than 1/2 drag count ($\Delta CD < 0.00005$).

The optimized wing T/C distribution when constrained to be at least 2.4% , closely matches the shape of the TCA T/C distribution. This indicates that for the selected airfoil shapes, the TCA is a very good design.

Effect of Wing Volume on TCA Optimization

Constraint: $T/C \geq 2.4\%$

Mach = 2.4



This shows the results of another optimization sensitivity study in which the wing volume was increased with the constraint that the local T/C must be at least 2.4% thick. For this study the wing volume is referenced to the volume of a $T/C = 2.4\%$ wing having the same airfoil shapes as the TCA. The thickness distributions and corresponding wing wave drags are shown for:

- Optimized wing with no T/C constraint
- Optimized wing with the constraint that T/C must be at least 2.4%
- Equal volume constant T/C wings.

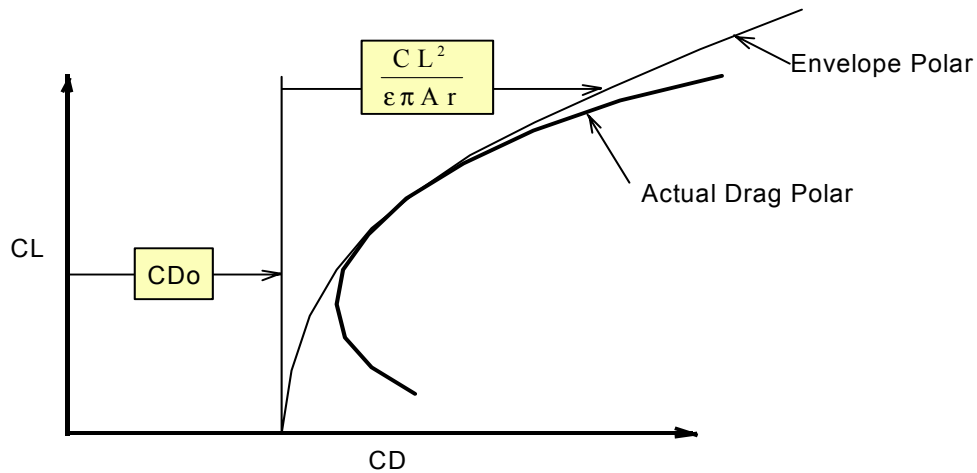
Again it is obvious that the optimized wings favor thick wing roots.

Notice that the drag of the constrained wing family passes through the TCA wing wave drag at the volume ratio equal to that of the TCA. Again indicating that the TCA baseline line is a good design for its airfoil shapes.

Subsonic Drag Polar Approximation

$$C_D = C_{D0} + \frac{C_L^2}{\epsilon \pi A r}$$

$$\left(\frac{L}{D}\right)_{\max} = 0.5b \sqrt{\frac{\epsilon \pi}{C_{D0} S_{ref}}}$$



We can approximate the subsonic drag polar by a simple parabolic equation.

$$C_D = C_{D0} + \frac{C_L^2}{\epsilon \pi A r}$$

C_{D0} is called the zero lift drag.

ϵ is the drag due to lift efficiency factor.

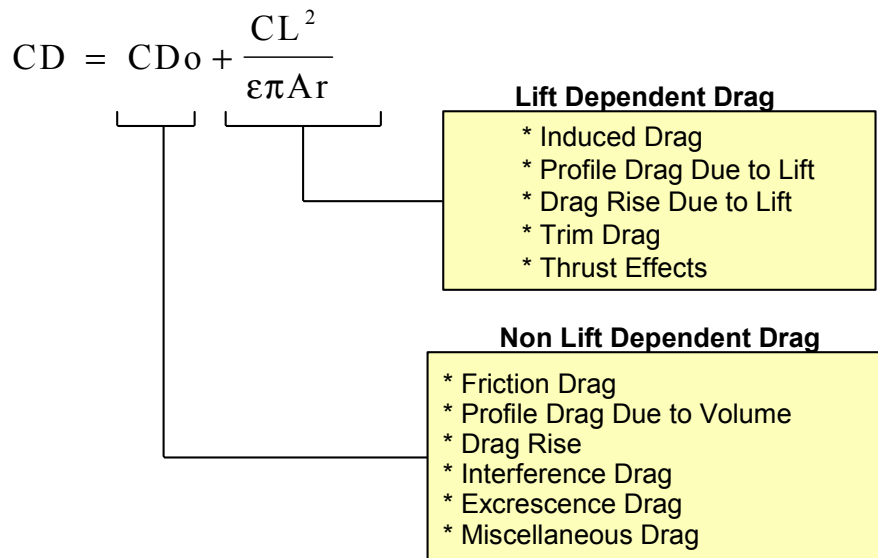
$A r$ is the wing aspect ratio,

Using this simple expression for drag, the L/D_{\max} value is given by a very simple expression.

$$\left(\frac{L}{D}\right)_{\max} = 0.5b \sqrt{\frac{\epsilon \pi}{C_{D0} S_{ref}}}$$

Subsonic Drag Components

$$\left(\frac{L}{D}\right)_{\max} = 0.5b\sqrt{\frac{\epsilon\pi}{C_{D0Sref}}}$$



The Non-lift dependent drag consists of:

- Friction drag
- Profile drag due to thickness.
- Compressibility drag
- Interference drag
- Excrescence drag and miscellaneous drag

The lift-dependent drag items include

- Induced drag
- Profile drag due to lift
- Compressibility drag due to lift
- Trim Drag

Tops Down L/D Analysis

- (L/D)_{max} at (M L/d)_{max} Subsonic Aircraft

Lower Bound Drag:

- Fully Turbulent Flow Friction Drag
- Elliptic Load Induced Drag $\epsilon=1$

$$C_D = C_{Fave} \frac{A_{wet}}{S_{ref}} + \frac{C_L^2}{\pi AR}$$

$$A_{wet\ adj} = A_{wet} \frac{C_{Fave}}{0.0021}$$

$$L/D\ max\ pot. = 19.34 \sqrt{\frac{b}{A_{wet\ adj}}}$$

For subsonic transport aircraft the lower bound drag components are usually considered to include:

- Minimum C_{Do} equal to fully turbulent flow flat plate skin friction drag.
- Minimum drag due to lift equal to the induced drag for planar wing configurations with elliptic load distributions.

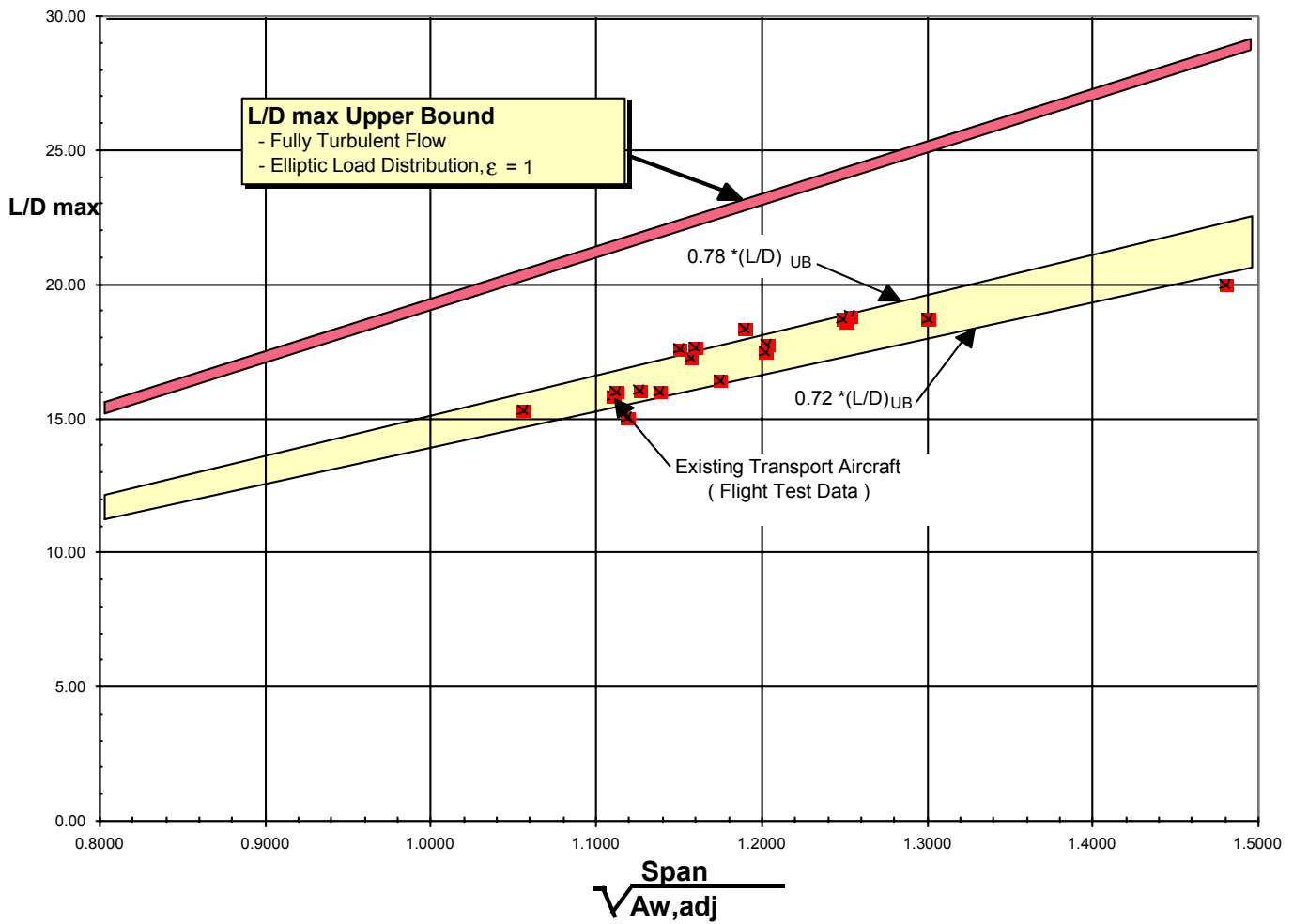
An adjusted wetted area is used to normalize out the effects of Reynolds number.

The adjusted wetted area is equal to the actual wetted area times the ratio of computed average skin friction coefficient to an average skin friction coefficient of 0.0021.

The “Tops Down” L/D max for subsonic transports is then equal to 19.34 times the wing span divided by the square root of the adjusted wetted area.

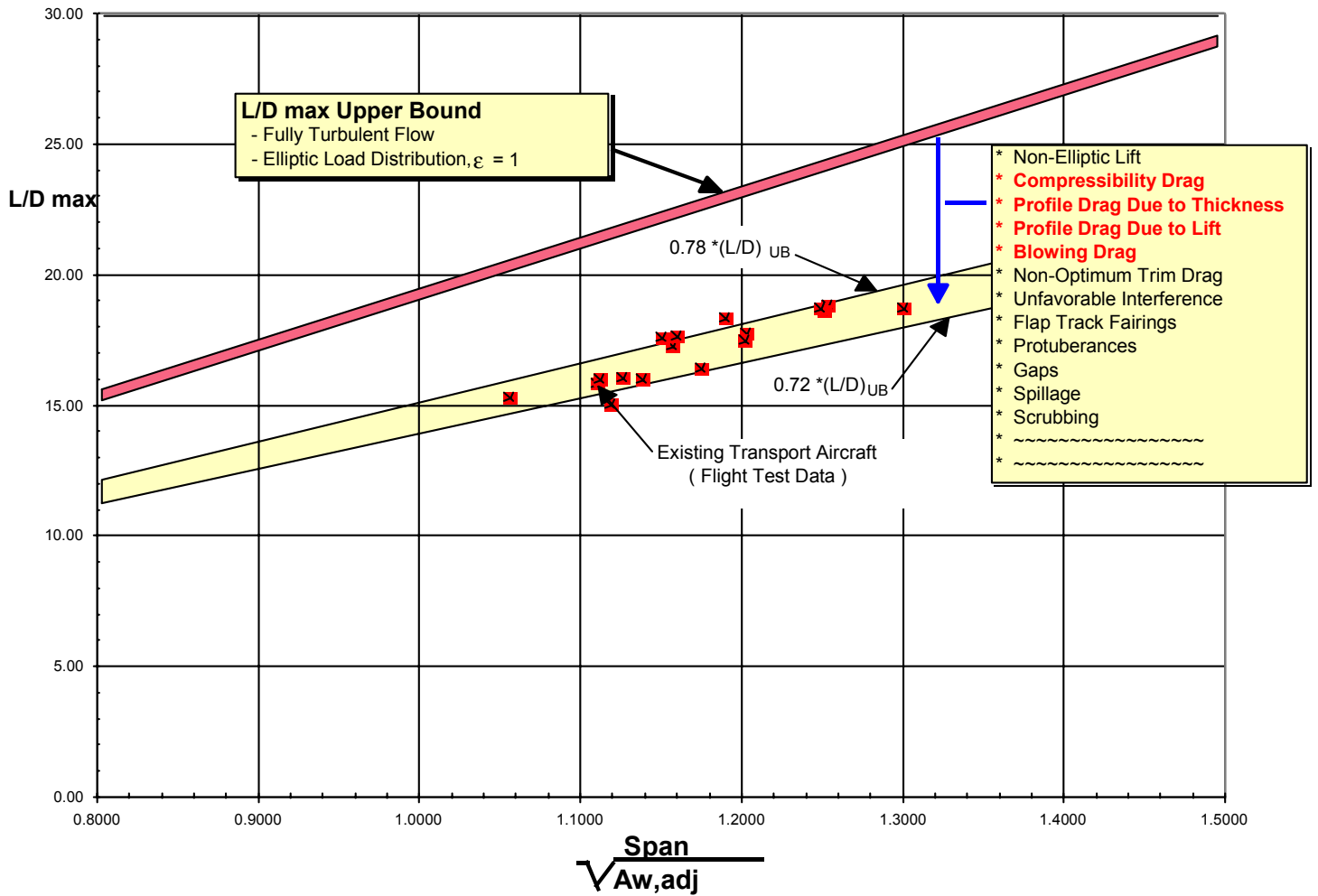
An “effective” span is used for aircraft having non-planar wing geometries such as tip fins. The “effective” span is the span of an equivalent planar wing that has the same induced drag as the non-planar wing.

Subsonic Transport Aircraft L/D max Potential



The values of L/D_{max} at the Mach number corresponding to $(M L/D)_{max}$ are shown for existing subsonic transport aircraft based upon flight test data. The existing aircraft achieve about 72% to 78% of the “achievable upper limit”

Subsonic Transport Aircraft Do Not Achieve L/D max Potential

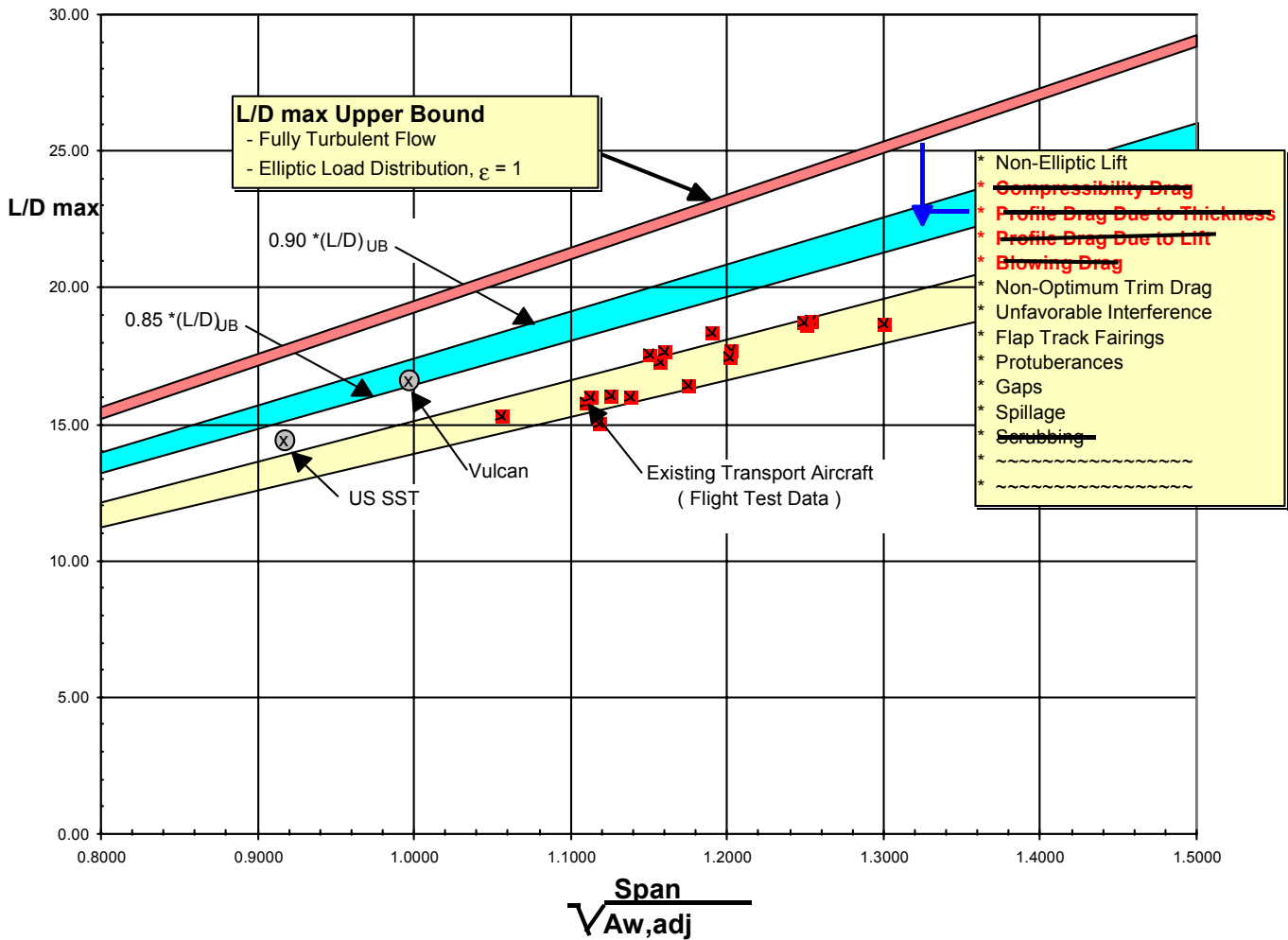


The Subsonic Configurations fail to achieve this Upper Bound Lift / Drag level because of a number of additional drag items as shown in the figure. The most Significant of these additional drag items include:

- The relatively thick airfoils and wide fuselages result in a profile drag increase over the viscous friction drag by approximately 20% to 25 %.
- At the long range cruise Mach number, subsonic aircraft typically have 15 to 20 counts of drag rise ($\Delta C_D = 0.0015$ to 0.0020).
- The spanwise load distributions based on structural design trades, tend to depart from the ideal load distribution. The typical spanwise load distributions are more heavily loaded near the wing root. This together with an increase in profile drag due to lift typically increases the induced drag approximately 10% to 12% above the ideal level.

These three drag items account for a 15% to 18% reduction in L/D from the Upper Limit L/D levels.

Low Aspect Ratio Subsonic Transport Aircraft L/D max Potential



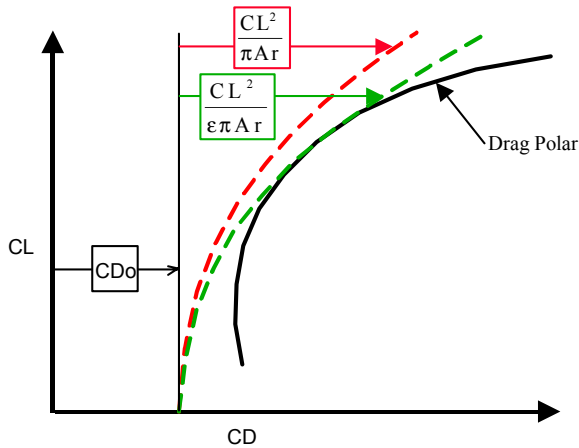
Supersonic type configurations tend to be long, thin and slender and cruise at relatively low lift coefficients. The subsonic viscous drag is essentially equal to flat plate skin friction drag.

The typical over land subsonic cruise Mach number for an HSCT of approximately 0.9 to 0.95. This is well below the drag rise Mach number.

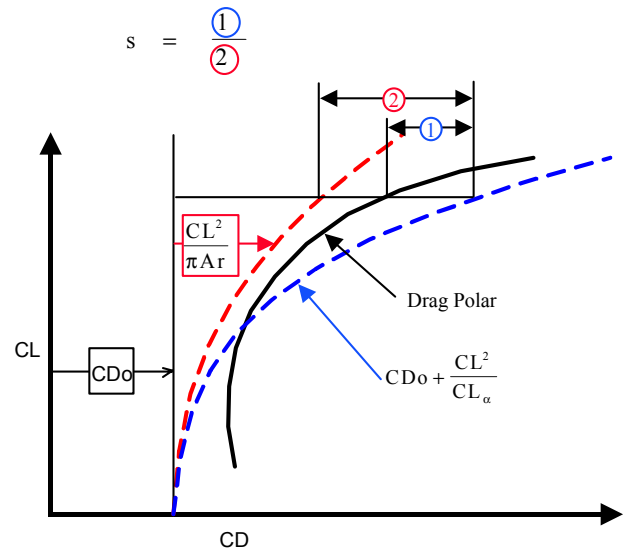
Consequently, it is expected that an HSCT operating with optimized flap settings should achieve L/Dmax values well in excess of the 80% of the corresponding upper bound levels demonstrated by existing subsonic transport configurations.

Subsonic Drag Polar Representations

Non-Elliptic Lift Factor: ϵ



Leading Edge Suction Factor: s



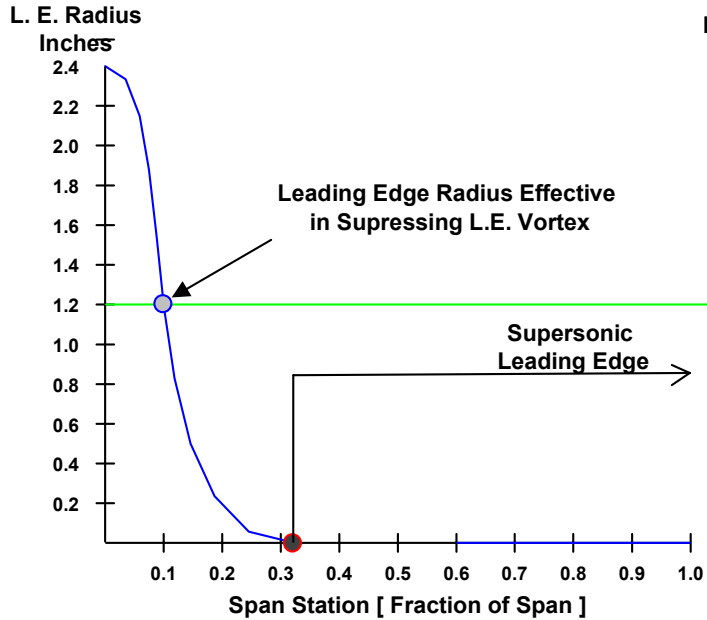
We will use a “bottoms up” approach to estimate the subsonic cruise L/D potential for the TCA configuration. It is convenient to consider two drag polar representations.

The first polar as previously discussed uses the drag due to lift efficiency factor, “ ϵ ”. This is useful for the “tops down” considerations.

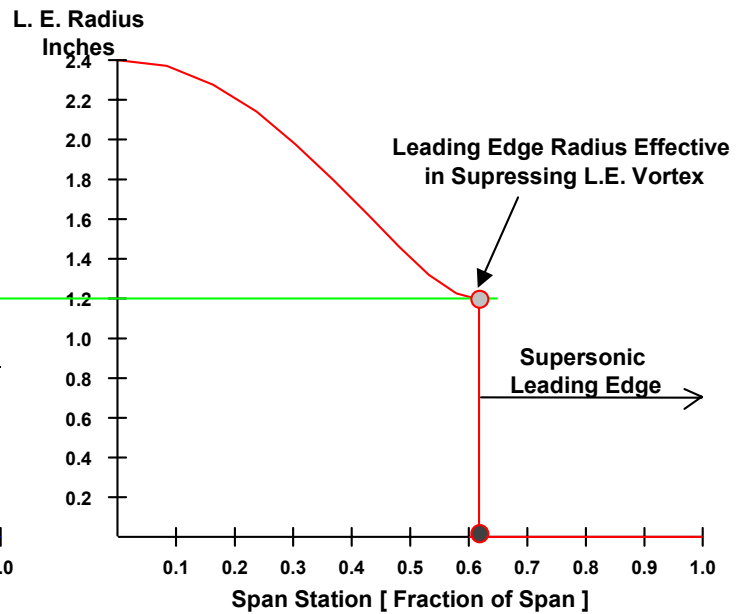
The second polar representation utilizes leading edge suction factor “ s ” which is defined here as the ratio of the “drag difference between the actual polar and the drag of a flat wing with zero suction” to the “drag difference between the ideal elliptic loaded wing and the drag of the flat wing with zero suction”. This is a more convenient representation for a drag build up approach.

Effect of Unique Bulbous Wing Leading Edge Radius Concept

Conventional Leading Edge Radius Distribution
US SST Design Concept



Bulbous Leading Edge Radius Distribution
TCA Design Concept



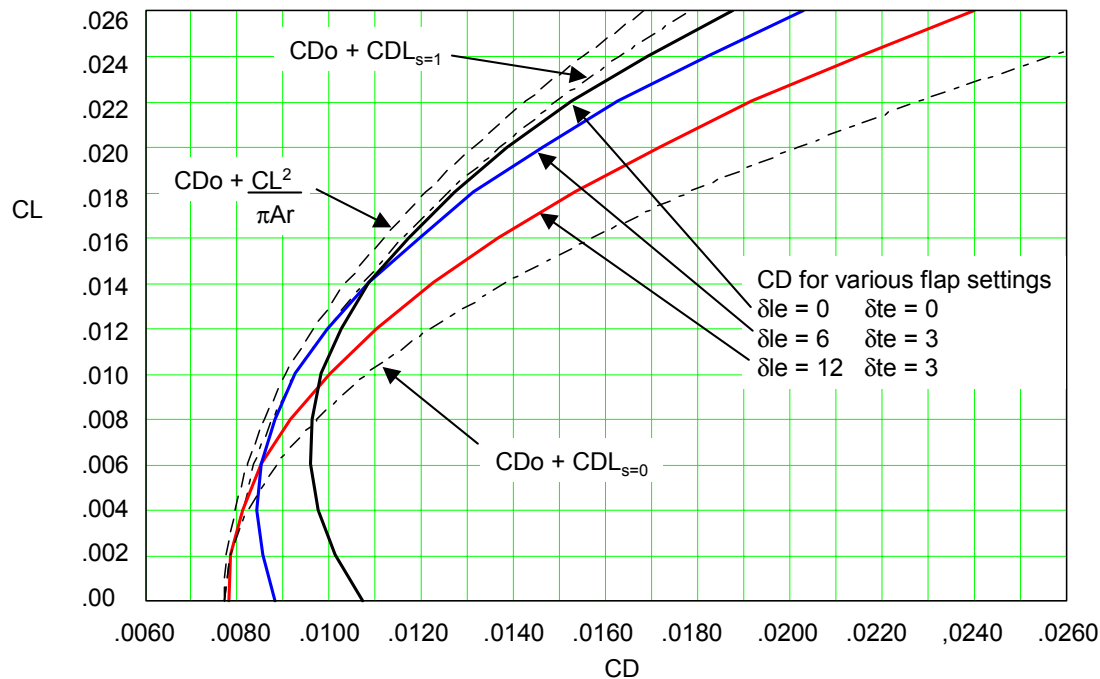
The current HSCT designs incorporate a bulbous leading edge radius design concept that was shown in the reference to reduce the drag due to lift of slender wing configurations.

Reference; Kulfan, R.M.; "Wing Geometry Effects on Leading Edge Vortices": AIAA 79-1872, August 1979.

Effect of Flaps on Subsonic Drag

HSCT Type Configuration

Mach = 0.9



This shows various predicted drag polars for an early HSCT configuration that utilized the large inboard leading radius concept.

The polars shown include:

- Minimum drag with an elliptic load distribution: $CD_0 + \frac{CL^2}{\pi Ar}$

CD_0 is equal to the flat plate skin friction drag plus a small profile drag correction corresponding to the reference symmetric equivalent configuration.

- Ideal drag with full suction for the actual cambered wing: $CD_0 + CD_{L_{s=1}}$

This wing geometry which was designed to minimize supersonic cruise drag generally does not have an elliptic load distribution at subsonic conditions.

- Reference drag for a thin flat wing with zero suction and developing no vortex lift:

$$CD_0 + CD_{L_{s=0}}$$

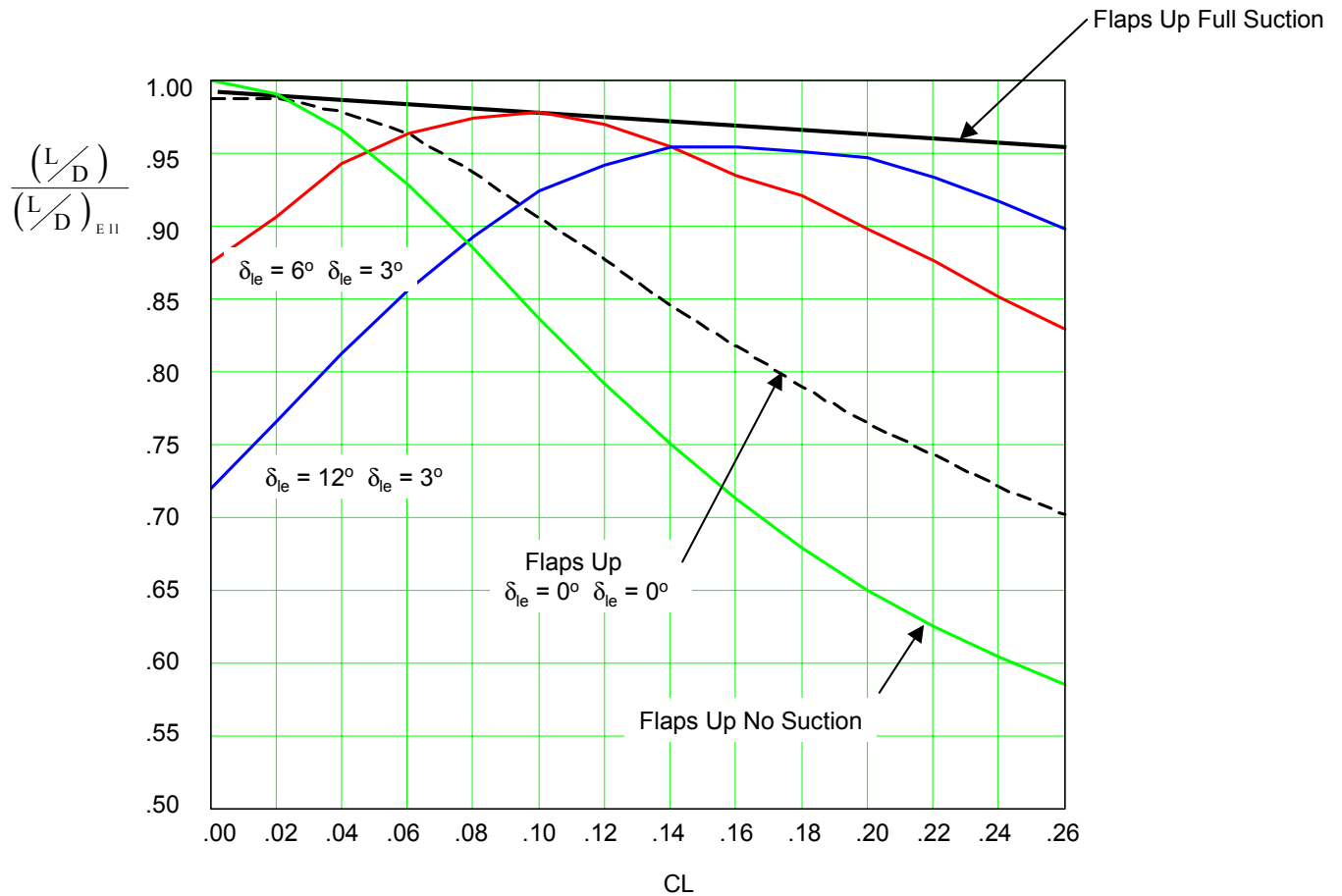
- Calculated polar shapes for the specified wing geometry for three near optimum flap deflections. The drag closely matches the ideal wing with full suction. At the design CL .

$$CD_0 + CD_{L_{\delta_{LE}, \delta_{TE}}}$$

Effect of Flap Deflection on L/D

HSCT Type Configuration

Mach = 0.9

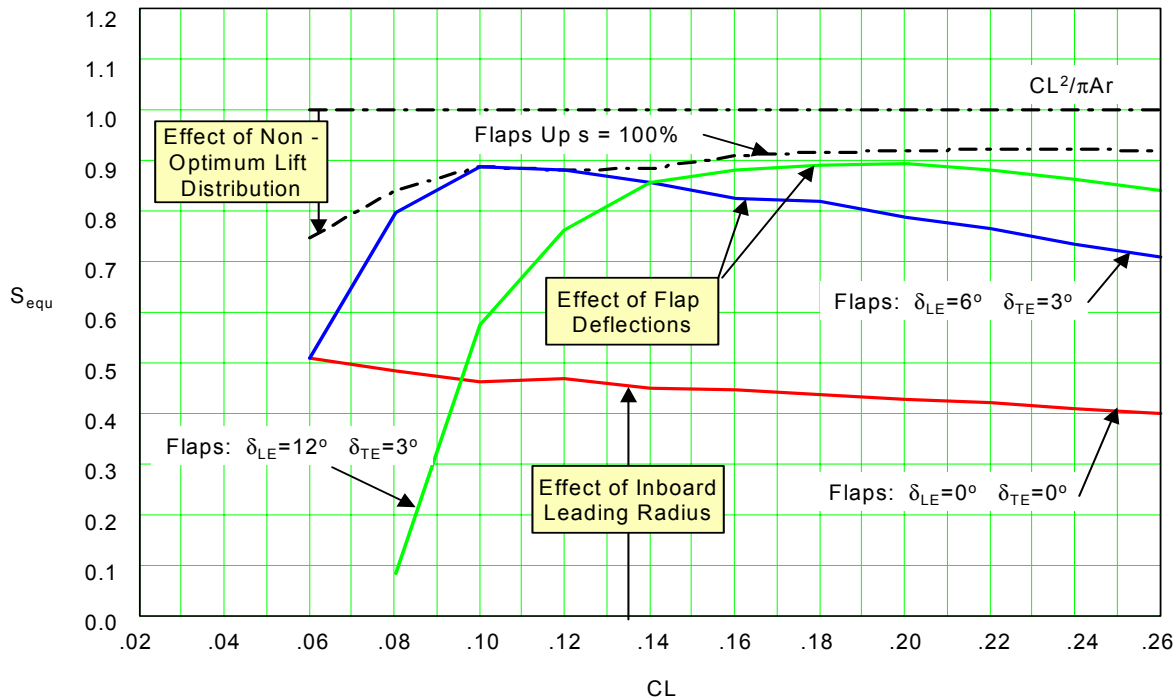


This shows the previous drag polar data plotted as the ratio of L/D of the configuration to the optimum L/D corresponding to an elliptic load distribution. It is readily apparent that flap deflections are essential to achieving good subsonic performance for an HSCT configuration.

Effect of Flap Deflections on Equivalent Suction Factor

HSCT Type Configuration

Mach = 0.9



The drag characteristics are shown here as “equivalent suction factors” S_{equ} as defined in the previous figure that compares the two polar representations, and by the equation:

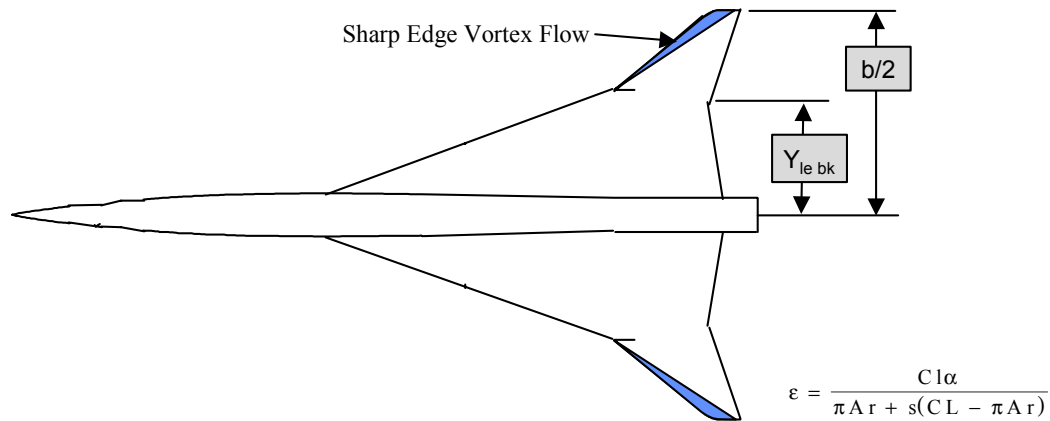
$$S_{equ} = \frac{CD_{S=0} - CD}{CD_{S=0} - CD_{ell}}$$

Where:

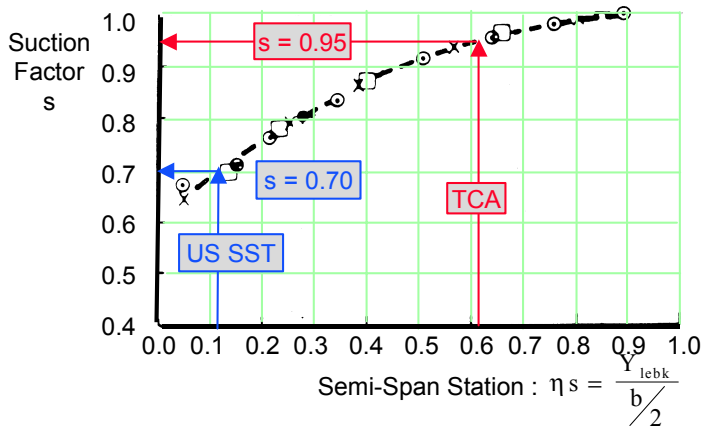
- $CD_{S=0}$ is the drag of the flat wing with zero suction
- CD_{ell} is the minimum drag with an elliptic load distribution
- CD is the drag of the wing with the specified flap deflections

The benefit of the round leading radius and flap deflections are both very important for high L/D.

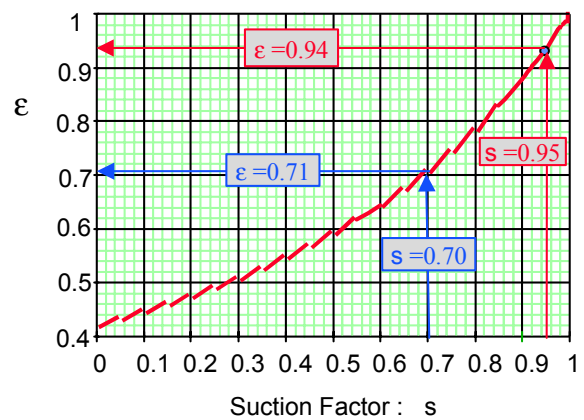
Effect of Leading Edge Vortex on Residual Suction



Effect of Outboard Leading Edge Vortex on Suction Factor



Span Efficiency Factor versus Suction Factor



The figure on the left is based on the wing geometry effects on leading edge vortex studies described in the reference. The leading edge suction factor at any angle of attack is dependent on the spanwise station for which the leading edge vortex is naturally suppressed by the basic airfoil geometry. Outboard of this station the wing is assumed to use flaps to suppress the vortex formation. The chart indicates the most outboard station on the TCA for which the the subsonic leading edge has a significant leading edge radius. The US SST is also shown. This implies that the TCA could achieve a suction factor of 0.95.

The chart on the right relates the suction factor “s” to the span load efficiency factor “ε” for the TCA. The suction factor of 0.95 corresponds to an “ε” = 0.94 which will be used in a bottoms up buildup of the TCA achievable L/D.

Reference; Kulfan, R.M.; “Wing Geometry Effects on Leading Edge Vortices”: AIAA 79-1872, August 1979.

TCA “Bottoms Up” L/D Projection

$$CD = CDF (1 + 0.8K_{\text{exces}}) + \frac{CL^2}{0.94\pi A_T} + CD_{\text{misc}}$$

Drag Components:

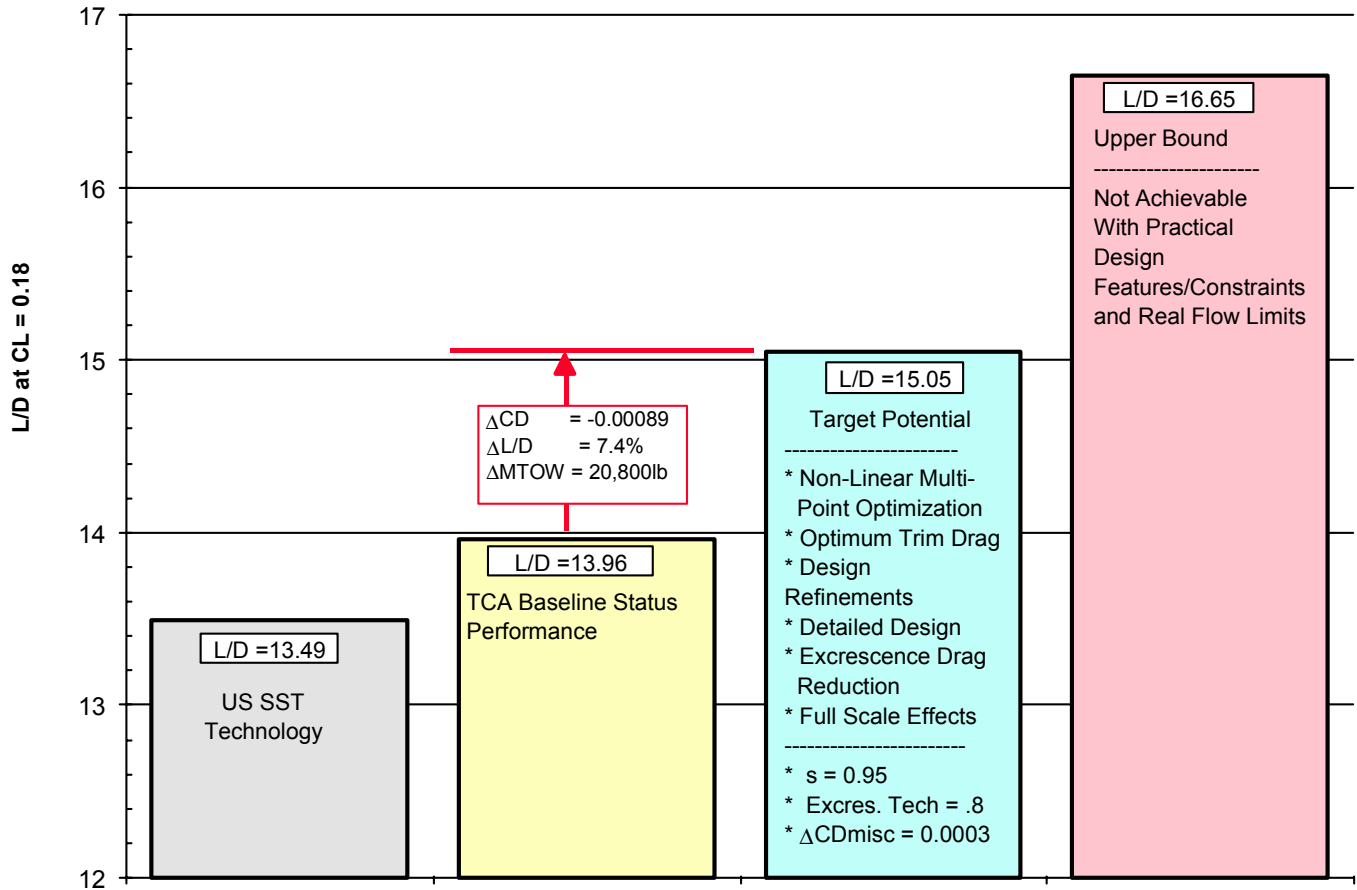
- Drag Due to Lift Corresponding to $S = 0.95 \implies e = 0.94$
- Excrescence Drag Reduction of 20% Relative to US SST
($K_{\text{exces}} = .095$)
- Fully Turbulent Flat Plate Skin Friction Drag
- $CD_{\text{misc}} = 0.0003$ (Propulsion Induced Effects, ??)

The achievable lower bound L/D potential for the TCA is composed of the following drag components:

- Drag due to lift corresponding to $\epsilon = 0.94$
- 20% excrescence drag reduction relative to the US SST because of the use of composite structure and improved manufacturing techniques.
- Fully turbulent flat plate skin friction drag.
- $CD_{\text{misc}} = 0.0003$ to account for such things as unavoidable pressure interference, propulsion induced effects, ???

TCA Subsonic Cruise L/Dmax Projections

Mach = 0.9 CL= 0.18

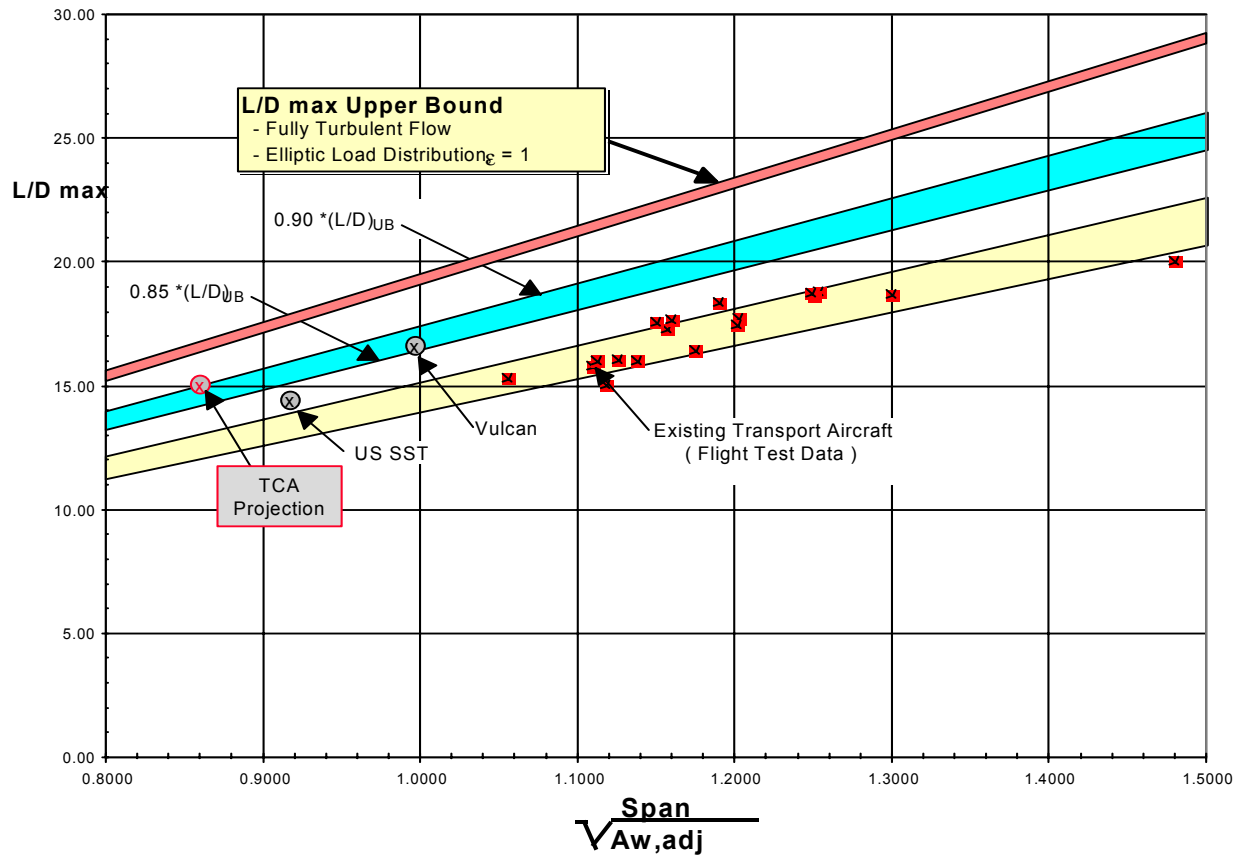


This compares the current performance level L/D of the TCA with the US SST technology, the “bottoms up” target potential and the “Tops down” upper bound for the TCA.

The projected drag reduction of -0.00089 corresponds to an L/D increase of 7.4%, This is equivalent to a max takeoff weight reduction of 20,800 lbs.

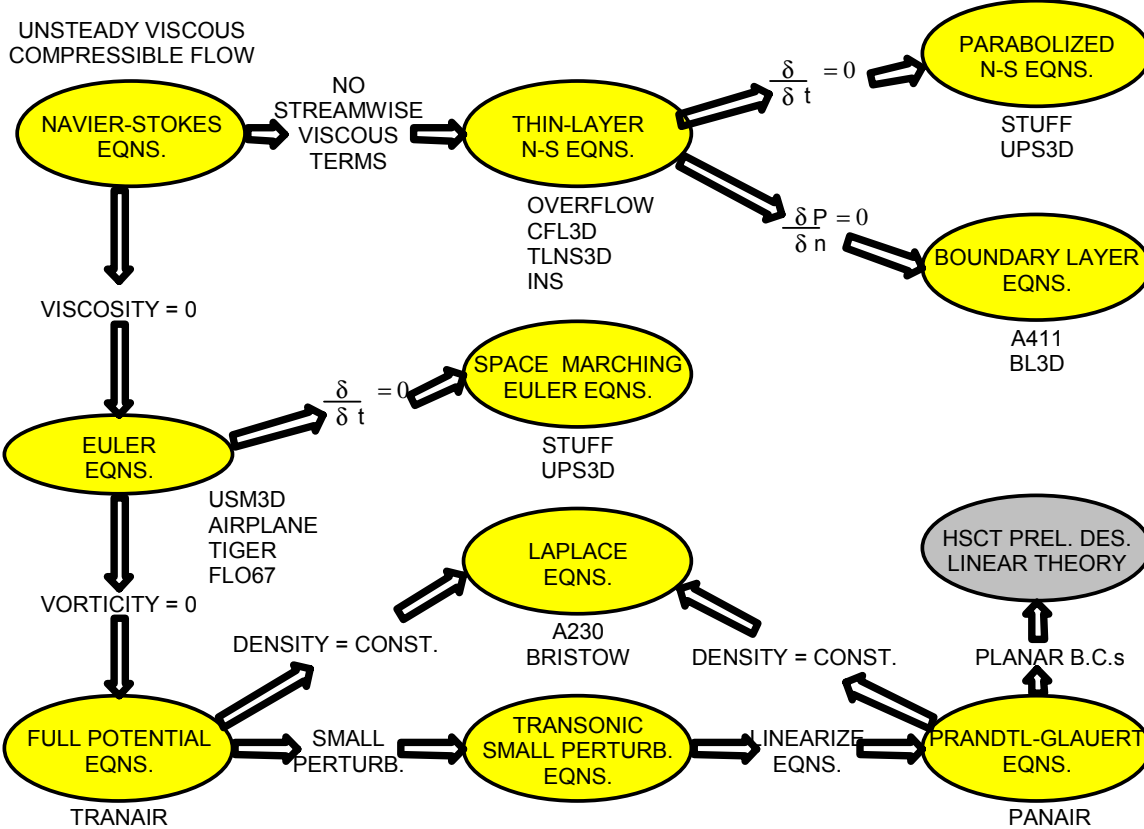
TCA Subsonic Cruise L/D max Potential

Mach = 0.9



The previously described TCA projection is shown to agree with what might be expected for a HSCT type configuration from a “tops down assessment”.

EQUATIONS OF FLUID DYNAMICS



The development and appropriate use of the advanced CFD design and analysis tools is important for developing a viable HSCT.

This shows the hierarchy of fluid dynamic equations starting from the unsteady viscous compressible flow Navier-Stokes equations.

The key assumptions in reducing the complexity of the equations to move to the next lower level are also shown.

Some of the various CFD codes in use by NASA and industry are shown next to basic set of equations that are solved by the codes. The Navier-Stokes flow solvers also can be used to solve the Euler equations.

The The HSCT preliminary design linear theory methods reside at the bottom of the hierarchy.

There are a number of simplifying assumptions that are inherent even in the Navier-Stokes equations. The Navier-Stokes equations assume that the fluid medium is a single component perfect gas that can be treated as a continuum in which stress is proportional to strain, and pressure is proportional to density times temperature.

Equations of Fluid Dynamics (continued)

Relative to the Navier-Stokes equations, the HSCT linear theory equations assume:

1. inviscid flow: The viscous effects are included in the skin friction drag. This requires care in applying the linear theory to avoid conditions leading to separated flow.
2. Irrotational Flow: The irrotational flow assumption greatly simplifies the numerics of a flow field solution since a single scalar equation is solved in terms of a velocity potential. The vector flow field can be obtained from the velocity potential scalar function. This limits the flow to moderate strength shocks, and non-rotational flow. However, these favorable flow conditions correspond to those on a low drag HSCT Configuration.
3. Small Perturbations. The Assumptions of small perturbations allows the velocity potential equations to be linearized. The solution process to becomes much easier. In addition, linearization allows the powerful concept of superposition to be used. This allows separation of the volume and the lifting effects and provides fundamental understanding of the flow phenomena. Again, the assumption of small perturbations is quite valid for HSCT low drag configurations which tend to be thin and slender, and operate at low lift coefficients.
4. Planar boundary conditions. The assumption of planar boundary conditions further simplifies the solution process. The sources / sinks and lifting elements that represent the geometry must lie on the axes of the fuselage, or the nacelles; and in the plane of the wing. These planar boundary conditions restrict the geometry to circular body and nacelle cross sections, and mid wing / body configurations. It is therefore easy to misapply the theory. In addition design details such as wing / body intersections or nacelle diverter geometry can not be analyzed directly.

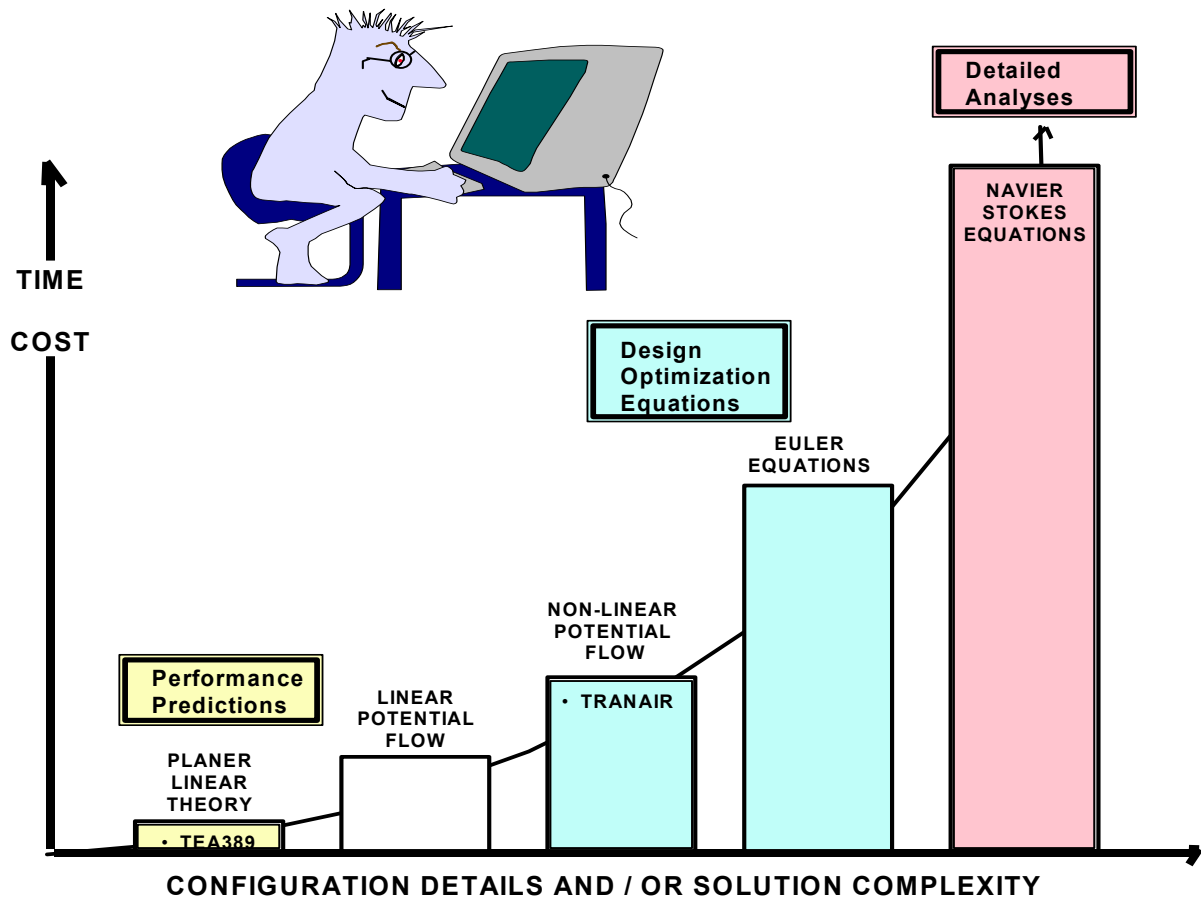
Elegant numerical and analytic solutions are possible. These solutions can provide insight and a fundamental understanding of key design variables, design sensitivities and potential performance levels.

The major difficulty with the planar boundary conditions is that numerical singularities can occur in the solution processes. The numerical analyses methods must properly treat these localized numerical singularities.

Currently, the linear theory methods most commonly used for designing optimum wing camber and twist, result in singularities in the camber / twist definitions. The smoothing process significantly reduces the potential benefits of camber optimization.

It is felt that non-linear optimization will be able to achieve drag benefits identified by the linear theory predictions but are unachievable by the linear designs.

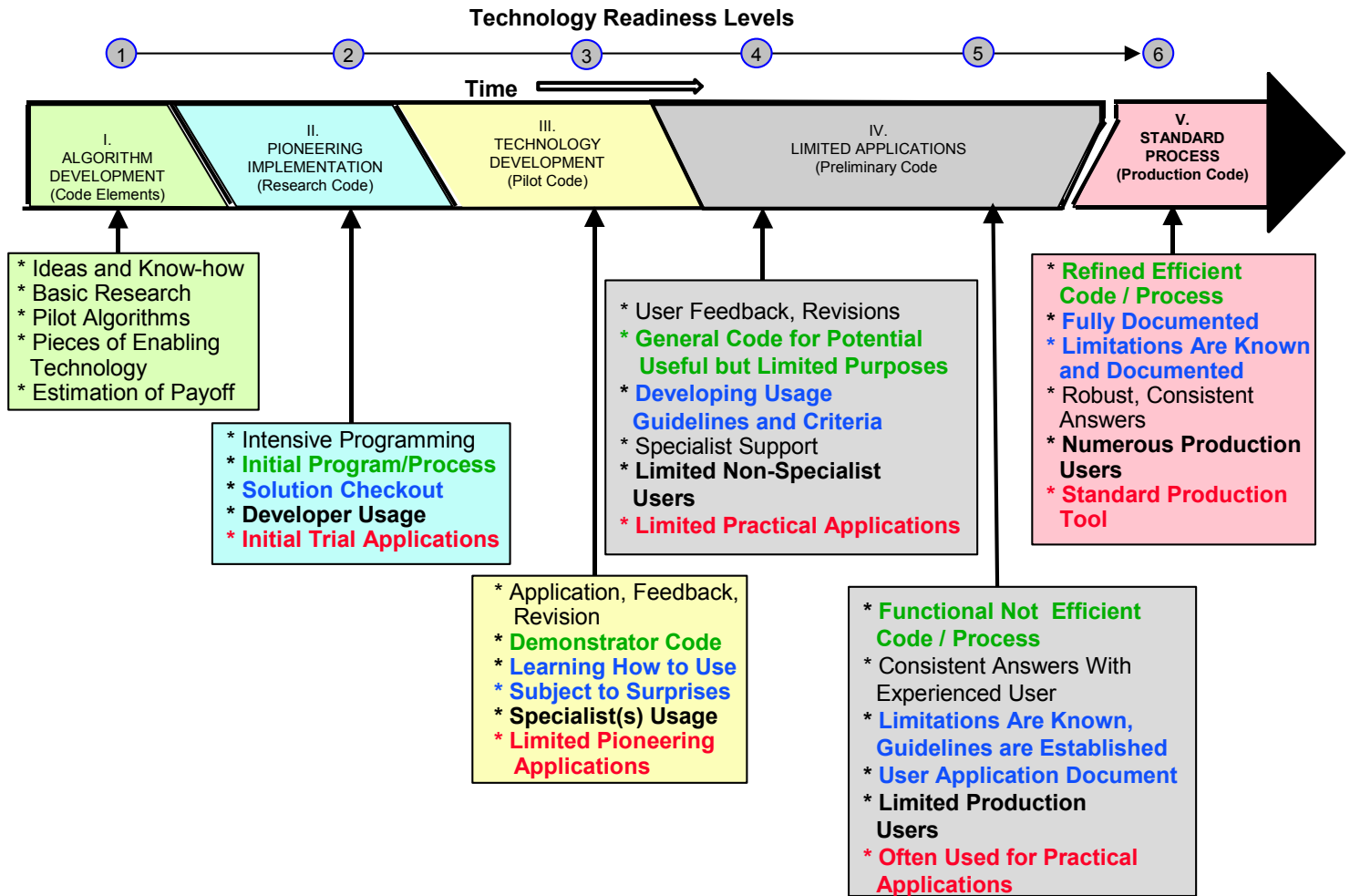
CFD ANALYSIS QUANTUMS



This illustrates the current impact on cost / solution time that is associated with the increased complexity of the CFD codes.

An important part of the CFD development and validation studies is to identify the appropriate tool to use for any specific application.

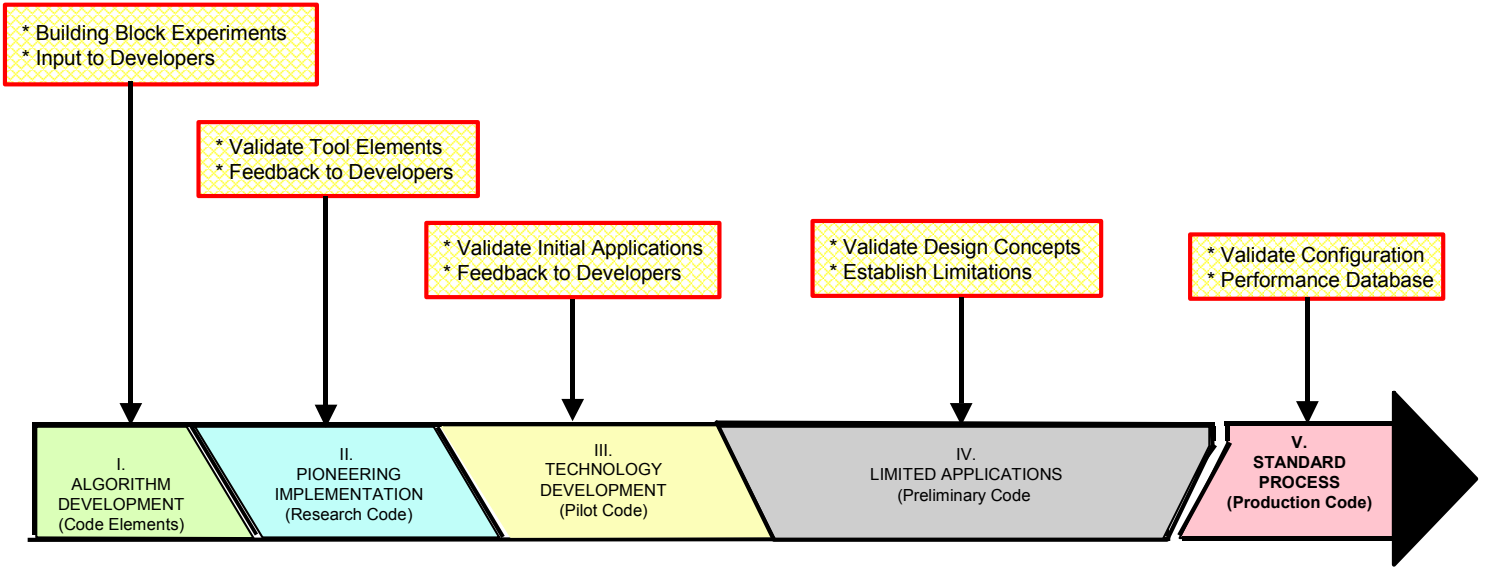
STAGES OF CFD DEVELOPMENT



This shows five typical stages of the CFD development process. I have attempted to relate the HSR technology readiness levels to the CFD development stages. The general features and capabilities of a CFD code are defined for each stage. These definitions can be used to track the development and validated application capability of the CFD codes.

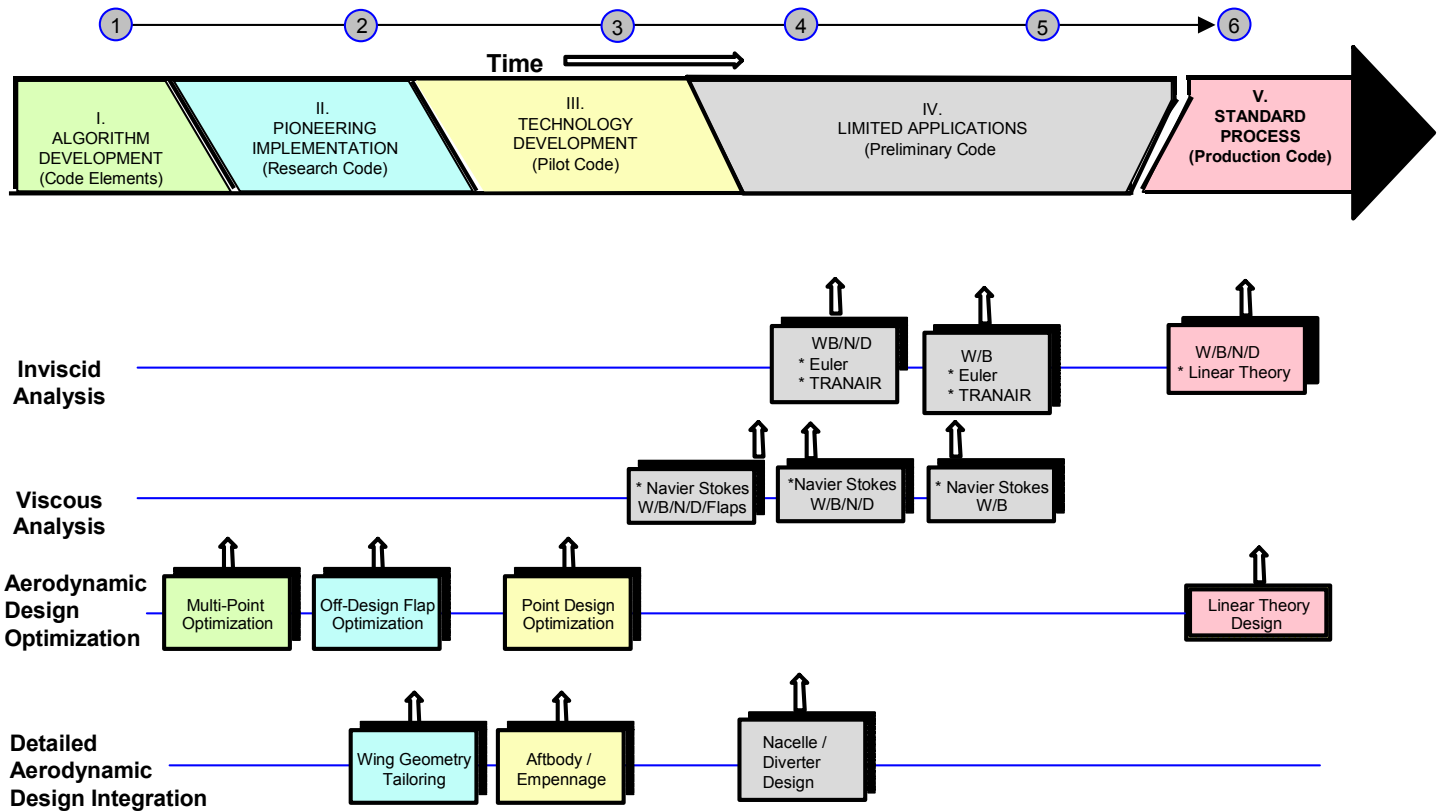
Required Wind Tunnel Testing in the Evolution of CFD Tools

SUPPORTING WIND TUNNEL OBJECTIVES



Wind tunnel testing plays an important part in the evolution of CFD tools. Validation wind tunnel experiments are necessary to allow movement of a CFD tool or particular application of a CFD tool through the development stages.

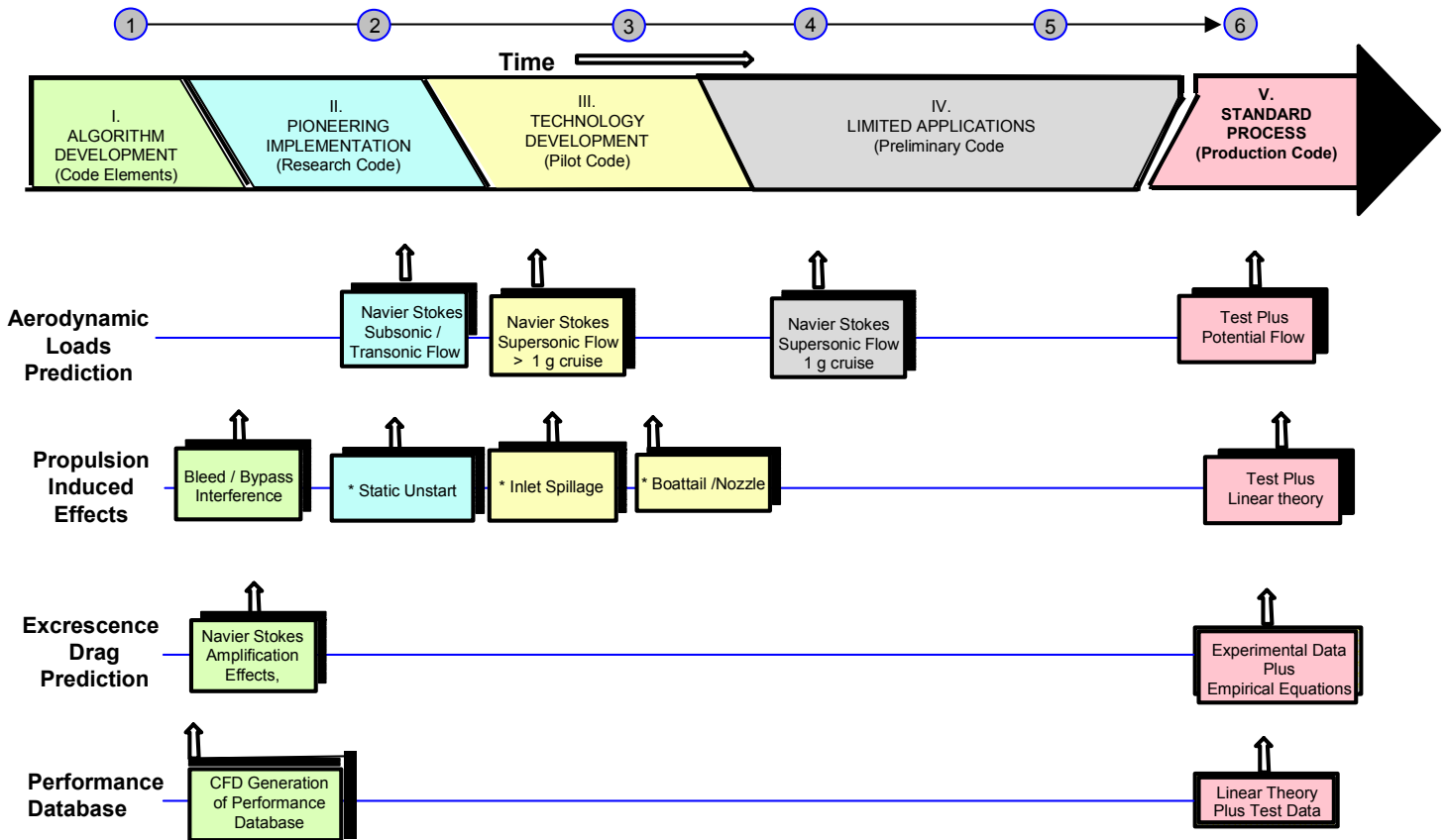
1996 HSCT CFD DEVELOPMENT STATUS



This is an assessment of the current state the CFD tools for:

- Inviscid analyses
 - Wing / body
 - Wing / body / nacelle /diverter
- Viscous analyses
 - Wing / body
 - Wing / body / nacelle /diverter
 - Wing / body / nacelle / diverter / flaps
- Aerodynamic design optimization
 - Point design optimization
 - Off-design flap optimization
 - Multi-point optimization
- Detailed Aerodynamic design integration
 - Wing geometry tailoring such as leading edge radius, wing body junctions, etc..
 - Aftbody empennage design
 - Nacelle / diverter / airframe integration

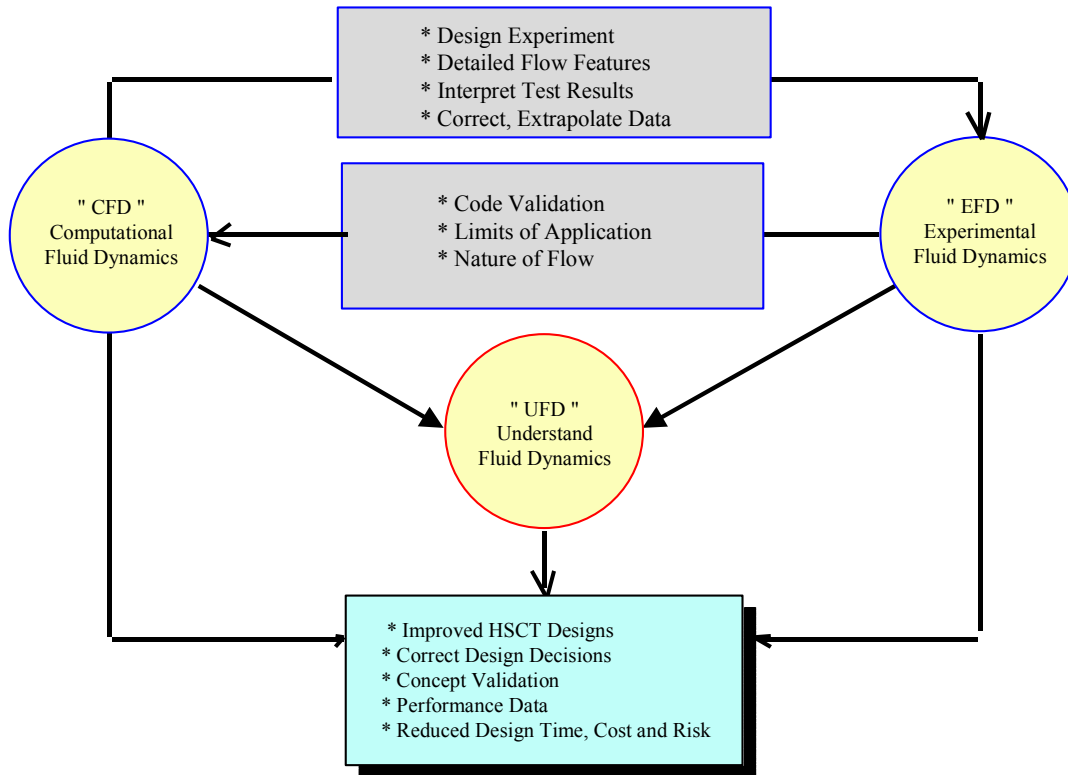
1996 HSCT CFD DEVELOPMENT STATUS



This is an assessment of the current status of CFD tools for other validated applications including:

- Aerodynamic loads predictions
- Prediction of propulsion induced effects
- Excrescence drag prediction
- Use of CFD to produce the extensive data base necessary for detailed airplane performance studies

INTEGRATED AERODYNAMIC TECHNOLOGY TOOLS



- "CFD" Computational Fluid Dynamics
- "EFD" Experimental Fluid Dynamics
- "UFD" Understanding Fluid Dynamics

These are used in an integrated development process as shown in the Figure.

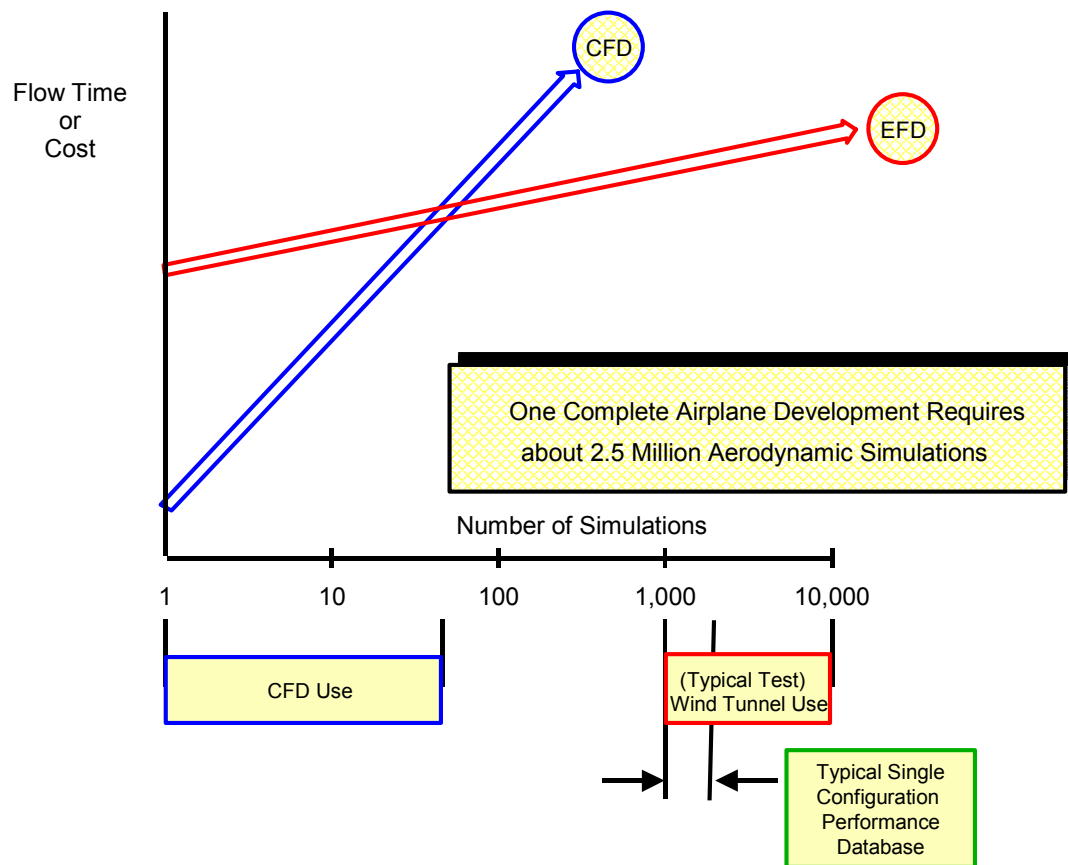
CFD is used to design our experiments, provide flow details to aid in the interpretation of the test results, and to correct and extrapolate the test data.

EFD results are critical for code validation, understanding the nature of the flow physics and to help identify the limits of application of the various CFD codes.

EFD and CFD provide vital information to develop our understanding of fluid dynamics. This is perhaps our greatest "tool"

UFD also assists in the planning, execution and understanding the results of any CFD or EFD activity.

Cost and Flow Time Characteristics of Wind Tunnels and CFD



This illustrates the relative cost and flow time characteristics of wind tunnel and CFD. It is obvious that CFD and EFD are both required elements in our aerodynamic tasks and processes.

It is very important to improve the efficiencies and quality of our CFD methods and EFD processes.

Summary and Conclusions

- **TCA Cruise L/Dmax Projections**
 - Current TCA Projection Appears Realistic
 - Modified Process Should Provide Greater Insight
- **TCA Subsonic Cruise L/Dmax Projections**
 - Current TCA Projection is Aggressive
 - Existing TCA Data will be Used to Benchmark Projections
- **Transonic / Low-Supersonic Projection Process**
 - Have None ---- Need One.
- **CFD Methods / Processes Development Assessment**
 - Significant CFD Developments Have Been Achieved
 - Number of Important Capabilities Have Not Been Validated
 - Current Design / Analysis Capabilities Are in Early Stages of Development

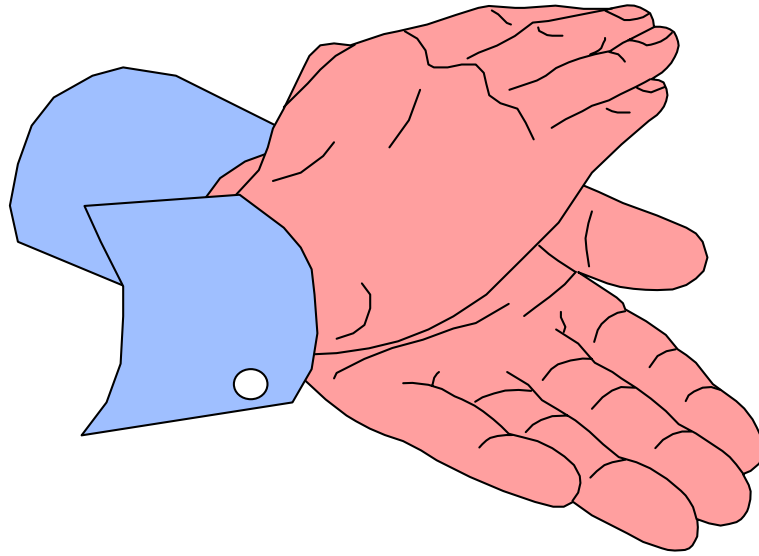
The TCA cruise L/Dmax projections appear realistic. It is expected that the modified process should provide greater insight into the projected performance potential. The modified process will also be useful for quick trade and sensitivity studies.

The TCA subsonic cruise projection is considered to be aggressive. The existing TCA data will be used to benchmark the status performance and refine the projections.

We currently do not have a process to predict off-design transonic/ low supersonic performance potential. A process is needed since this portion of the flight regime could have implications on the selection of the best engine cycle and could also impact the basic planform features.

All though substantial progress has been made in the development, application and validation of our CFD tools, many capabilities have either not been validated, or are in early stages of development.

Applause



This final figure is dedicated to all of the Configuration Aerodynamic Team members from NASA and Industry not only for their technical achievements, but also for their efforts and dedication that made these achievements possible.